#1039

PITHA 91/17
October 1991

QCD Studies at LEP

Thomas Hebbeker

III. Physikalisches Institut der Technischen Hochschule
Aachen
D-5100 Aachen, Germany

Plenary talk given at the

International Lepton-Photon Symposium
and
Europhysics Conference on High Energy Physics
July 1991

QCD STUDIES AT LEP

THOMAS HEBBEKER
*Phys. Inst. III A, RWTH Aachen, D-5100 Aachen, Germany**

ABSTRACT

Hadronic decays of the Z^0 produced in e^+e^- annihilation are ideal for precise tests of Quantum Chromodynamics. The experiments ALEPH, DELPHI, L3 and OPAL at LEP have observed in total more than a million hadronic events and have performed a large number of measurements. The most important results are: (a) The strong coupling constant is $\alpha_s(M_Z) = 0.120 \pm 0.007$. The energy dependence of the 3-jet fraction measured in e^+e^- annihilation between 20 and 90 GeV shows that α_s is running as predicted by QCD. (b) Second order QCD matrix element calculations reproduce all measured distributions for *jets* in 3-jet and 4-jet events. There is direct experimental evidence for the gluon self interaction. (c) All measured distributions for *hadrons* can be reproduced by QCD Monte Carlo programs or analytical calculations.

1. Outline

A large number of measurements of hadronic Z^0 decays and of tests of QCD have been performed. In this review only parts of the material can be presented. For each of the main topics I will show, as an example, the measurements of *one* LEP experiment and then compare and summarize the results of all experiments.

Here I consider only QCD tests based on the process $e^+e^- \rightarrow$ hadrons. The experimental results on the production and decay of heavy flavors (charm, bottom) are described in ref. [1]. Theoretical aspects of QCD are discussed in ref. [2].

After a brief introduction (section 2) and a description of QCD models (section 3) I review in section 4 the different measurements of the strong coupling constant α_s. Also studies of the flavor independence and of the running of α_s are presented. Detailed QCD tests based on 3-jet and 4-jet events, and in particular the measurement of the three-gluon coupling are described in section 5. 'Soft' phenomena such as particle spectra and string effect are the topic of section 6. Finally the prospects for future QCD studies at the Z^0 resonance are outlined in section 7.

2. Introduction

Quantum chromodynamics (QCD) is *the* theory of strong interactions. It is a nonabelian gauge theory with a SU(3) group structure describing the interaction of colored quarks with colored gluons. The basic Feynman graphs are shown in figure 1.

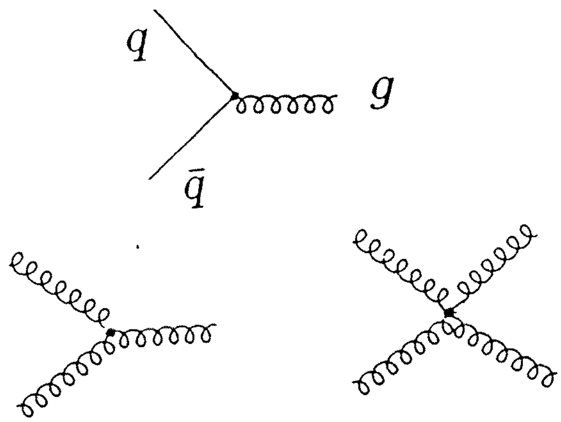

Figure 1: Basic Feynman diagrams in QCD

The only free parameter is the strong coupling constant α_s. It has a characteristic energy dependence as shown schematically in figure 2, which is often referred to as the 'running' of α_s. With increasing energy the coupling strength decreases ('asymptotic freedom'). This is a consequence of the gluon self interaction. For high energies the coupling constant is therefore sufficiently small

*supported by the German Bundesministerium für Forschung und Technologie

such that perturbative calculations can be performed. For low energies the coupling constant becomes large, which is believed to be the origin of confinement.

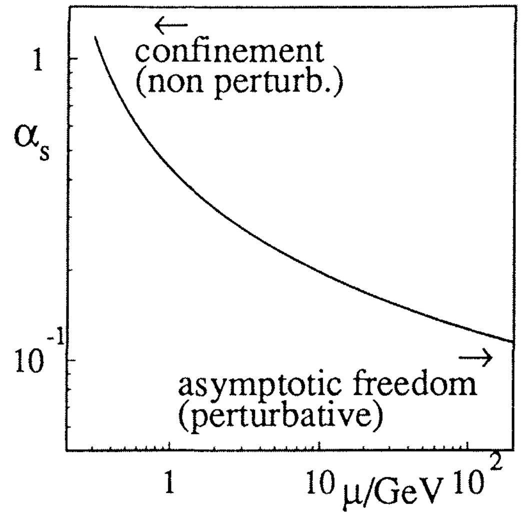

Figure 2: Running of α_s

The process $e^+e^- \to$ hadrons at high center of mass energies is well suited for QCD tests: The initial state is well defined. The high momentum quarks and gluons (figure 3) form jets, tight bundles of hadrons, which preserve the energy and the direction of the primary partons to a good approximation.

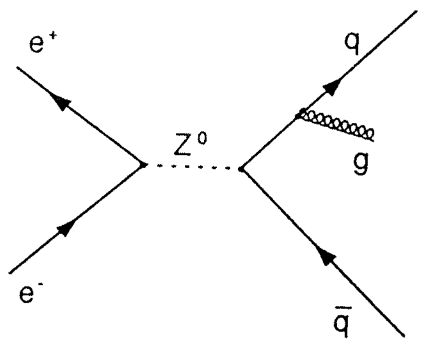

Figure 3: $e^+e^- \to q\bar{q}g$

Important features at $\sqrt{s} = 91.2$ GeV in comparison with $\sqrt{s} \approx 30$ GeV (PEP, PETRA) are:

- higher center of mass energy $\sqrt{s}$,
- relatively small fragmentation effects,
- large cross section (≈ 30 nb) and negligible background (typically $\ll 1\%$),
- hard initial state photon radiation suppressed,
- different flavor composition (up/down ≈ 1 instead of ≈ 4).

Therefore one finds at the Z^0 pole a large number of events with 2, 3 and 4 well collimated jets with an energy exceeding 10 GeV. These 'clean' topologies allow for a precise determination of α_s and for many tests of QCD.

The LEP experiments ALEPH [3], DELPHI [4], L3 [5] and OPAL [6] each have observed about 250,000 events $e^+e^- \to Z^0 \to$ hadrons in the period up to July 1991.

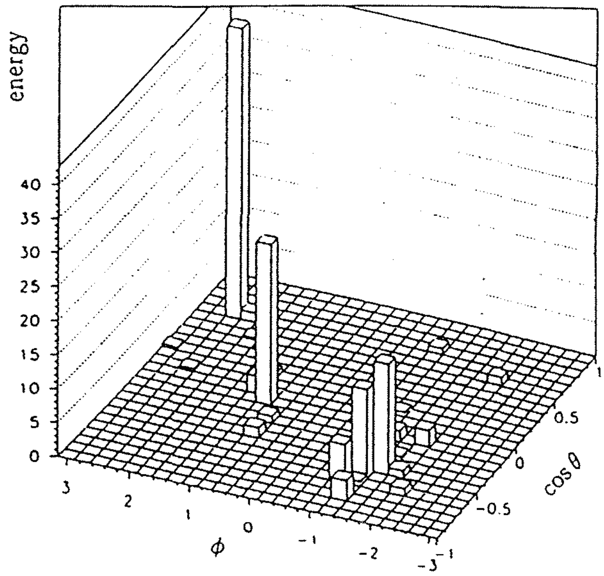

Figure 4: 'LEGO-plot' of a 3-jet event (L3)

All detectors allow for the measurement of charged tracks and are equipped with fine grained calorimeters measuring the energy flow of charged and neutral particles. The detectors are almost hermetic and are thus well suited for precise measurements of hadronic events.

Figure 4 shows a 'Lego plot' of a hadronic event obtained at 91 GeV center of mass energy. It shows nicely that the jets are narrow and well separated from each other.

3. QCD models for $e^+e^- \to$ hadrons

One can distinguish four separate phases in the process $e^+e^- \to$ hadrons. They correspond to different time scales and are sketched in figure 5 [7].

(i) Production of a $q\bar{q}$ pair (and photons) [electroweak]

(ii) 'Hard' gluon radiation [perturbative QCD]

(iii) Fragmentation of quarks and gluons into hadrons [non-perturbative QCD]

(iv) Decays of unstable particles [electroweak and QCD]

These subprocesses are implemented in Monte Carlo event generators [7], which play an important role in the analysis of hadronic events.

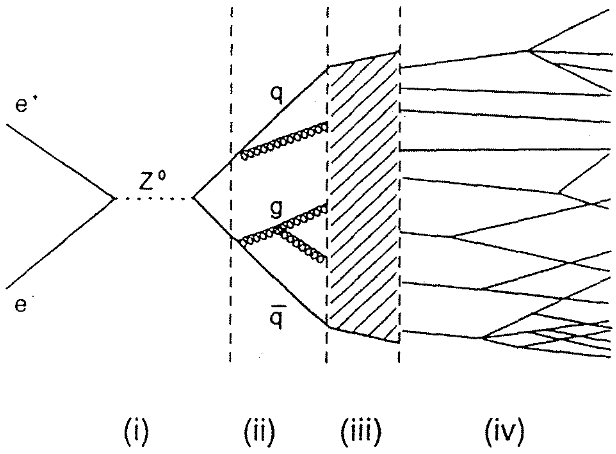

Figure 5: The process $e^+e^- \to$ hadrons

Phase (ii) is of primary interest here. It can be calculated perturbatively within QCD and allows for quantitative tests. There are two approaches:

- 'Matrix elements' (exact 2^{nd} order calculation),
- 'Parton showers' (leading log approximation).

Matrix element based event generators produce up to 4 partons with a minimum invariant mass m of two partons of about 10 GeV at the Z^0 resonance. Some of the corresponding Feynman diagrams are shown in figure 6 [7]. In addition there is a large number of graphs with virtual corrections.

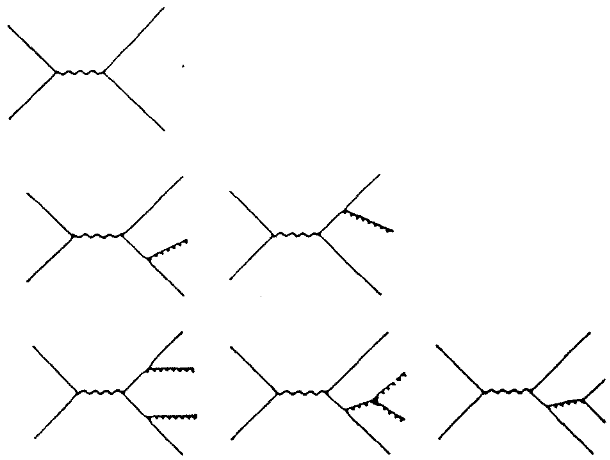

Figure 6: Feynman diagrams for $e^+e^- \to$ quarks and gluon(s) to $O(\alpha_s^2)$

In a parton shower on average 9 partons are generated at the Z^0 pole with virtual gluon masses m as low as $\approx$ 1 GeV, see figure 7 [7, 8].

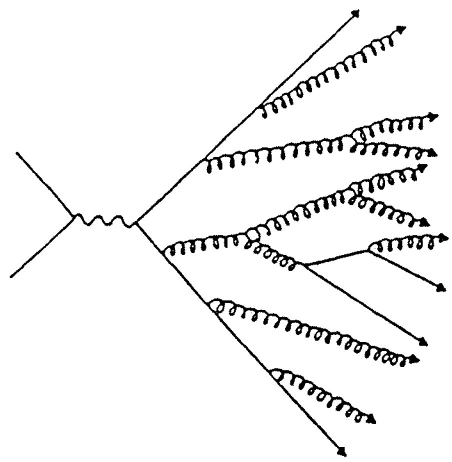

Figure 7: $e^+e^- \to$ quarks and gluons, parton shower approach

While in general parton shower generators reproduce measured distributions better, the matrix elements are needed for a determination of α_s, because only in the exact order by order calculation the strong coupling constant is well defined. Also for studies of jet distributions in multi-jet events they are needed, because of the correct hard parton kinematics in matrix element calculations.

The fragmentation of quarks and gluons, phase (iii), can be modeled quite successfully by string and cluster fragmentation schemes [7]. In an event on average 17 hadrons are created which decay into a total of about 45 particles with a lifetime exceeding 10^{-9} s.

To be able to interpret measurements one has to use models to describe the hadronization process and also the subsequent decays. Therefore tuning and testing of fragmentation models is the first step in any analysis.

The most popular 'models' (i.e. Monte Carlo generators of hadronic events) are:

- JETSET [8]. Both parton shower and $O(\alpha_s^2)$ matrix element options are available [9, 10]. Most often the string fragmentation model is used.
- HERWIG [11]. This parton shower generator simulates spin and interference effects in detail. Hadronization is simulated by cluster fragmentation.

Other programs being used are ARIADNE [12], NLLJET [13], and the matrix element generator ERT-E_0 [9, 14].

To fit the parameters of the various models the following analysis steps have to be made:
1) Out of many free parameters in the model the relevant ones have to be identified.
2) Choice of distributions. Global event shape variables like thrust and oblateness or inclusive distributions as particle momenta are suitable [15].
3) Global fit to several distributions. The data, corrected for detector effects, are directly compared to the Monte Carlo predictions, and the relevant parameters are determined.

After the models are tuned they can be tested by comparing the predictions for event shape variables, in particular for those not used in the parameter fit, to the measurements. Figure 8 shows as an example the ALEPH thrust distribution in comparison with the predictions of the JETSET (both parton shower and matrix element) and HERWIG event generators [16].

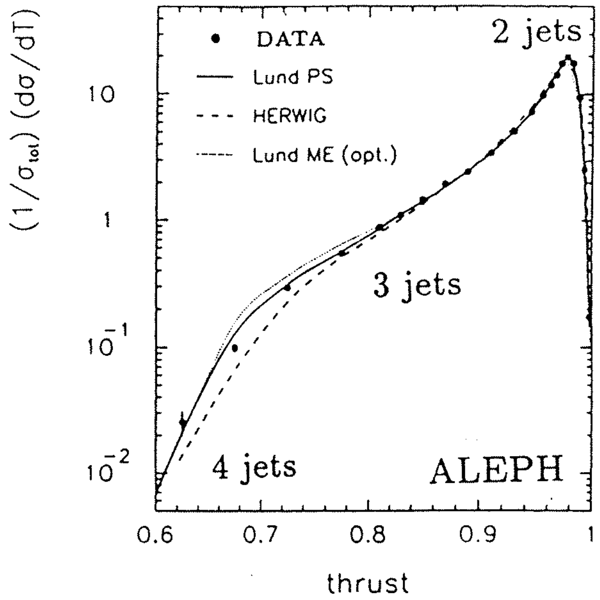

Figure 8: Distribution of Thrust T as measured by ALEPH in comparison with QCD models

Also DELPHI [17], L3 [18], OPAL [19] and MARK II [20] have compared measured event shape variables to model predictions and to measurements at lower center of mass energies.

The different studies arrive at similar results, which can be summarized this way:

- All models listed above can be tuned to describe hadronic Z^0 decays. Parton shower generators perform best.
- Parton shower models tuned at $\sqrt{s}$ = 91 GeV can also describe 30 GeV e^+e^- data.

Here we have considered global event properties obtained by analyzing the full hadron data sample with contributions from all flavors. For the heavier quarks charm and bottom, which can be tagged for example via their semileptonic decays, interesting measurements of their fragmentation properties have been made. They are reviewed in ref. [1].

4. Strong coupling constant α_s

There are many compelling reasons for measuring the strong coupling constant:

(1) α_s is the only free parameter in QCD,

(2) many tests of QCD require α_s to be known,

(3) for many electroweak tests strong corrections must be calculated precisely,

(4) grand unification theories can be tested by extrapolating the different coupling constants to very high energies [21, and references therein].

Apart from measuring the fundamental parameter α_s several tests of QCD can be made by comparing α_s values obtained from different variables (*consistency*), for different quark species (*flavor independence*), at different energies (*running*), and in different reactions (*universality*).

The strong coupling strength can be expressed either in terms of $\alpha_s(\mu)$ at an energy scale μ, or by using the QCD parameter Λ. The two equivalent quantities are related in next to leading order by [22]

$$\alpha_s(\Lambda,\mu^2) = \frac{1}{b_0 \cdot \ln(\mu^2/\Lambda^2)} - \frac{b_1}{b_0^3} \cdot \frac{\ln\ln(\mu^2/\Lambda^2)}{(\ln(\mu^2/\Lambda^2))^2}$$

where

$$b_0 = (33-2n_f)/(12\pi) \qquad b_1 = (153-19n_f)/(24\pi^2)$$

with $n_f = 5$ and $\Lambda \equiv \Lambda^{(5)}_{\overline{\rm MS}}$. In the past often Λ was used as the fundamental parameter in QCD due to a lack of a 'natural' energy scale $\mu_0 \gg \Lambda$ for which $\alpha_s(\mu_0)$ is small. Today we have a convenient reference scale $\mu_0 = m_Z$ and I will express the QCD coupling strength in terms of $\alpha_s \equiv \alpha_s(M_Z)$ (and not Λ) from now on.

In subsections 4.1 to 4.4 the measurements of the strong coupling constant in $e^+e^- \to Z^0 \to$ hadrons are described. The results of the QCD tests as listed above are summarized in subsections 4.5 to 4.7.

4.1. Measuring α_s in $e^+e^- \to Z^0 \to$ hadrons

There are two different methods to determine α_s:

1) Measurement of the hadronic partial Z^0 width $\Gamma_{\rm had}$ or, equivalently, of the hadronic cross section at the Z^0 pole. This implies counting of events. The QCD correction to the hadronic width has been calculated to third order in α_s [23], and the uncertainty due to missing terms of $O(\alpha_s^4)$ is presumably small. There are no hadronization uncertainties, since the fragmentation process can only change the shape of an event, but can not make it disappear. (For a possible effect of final state interference see ref. [24].) Since the QCD correction ($\approx \alpha_s/\pi \approx 4\%$) is small, a very high experimental precision is required: In order to reach $\Delta\alpha_s = 0.01$ an accuracy of $\Delta\Gamma_{\rm had}/\Gamma_{\rm had} = 0.3\%$ is needed.

2) Analysis of the event topology, in particular a study of events with hard gluon bremsstrahlung. The fraction of those events is to lowest order proportional to α_s. A large number of variables exist to measure the hard gluon content in hadronic events [15]. Here I will concentrate on jet fractions, from which the strong coupling constant can be obtained with relatively small hadronization uncertainties. Since the matrix element calculations for the 3-jet fraction and other event shape variables have been performed only to $O(\alpha_s^2)$, the uncertainty due to unknown higher order corrections is the dominant contribution to $\Delta\alpha_s$ in this method.

meth.	theoret. error high.O	theoret. error fragm.	experim. error	total uncert.
1)	2%	-	10-15%	10-15%
2)	5-10 %	3%	3%	5-10%

Table 1: Relative uncertainties for α_s.

These two methods are largely independent and therefore complementary. The theoretical and experimental uncertainties are quite different in both cases, as is shown in table 1. The theoretical error has two contributions: Missing higher order terms in the perturbative expansion and non-perturbative effects ('fragmentation'). The experimental uncertainties are the combined errors for all LEP experiments.

4.2. Determination of α_s from $\Gamma_{\text{had}}/\Gamma_{\text{lep}}$

The QCD correction to the hadronic width can be measured best from the ratio of the hadronic and leptonic partial widths of the Z^0 boson. It is given in the Standard Model by

$$R_Z \equiv \Gamma_{\text{had}}/\Gamma_{\text{lep}} = 19.97 \cdot (1 + \delta_{\text{QCD}}) \, .$$

The factor $\Gamma^0_{had}/\Gamma_{lep} = 19.97 \pm 0.03$ [25] depends only little on the top and higgs masses, since most m_t and m_H dependent corrections are common to Γ^0_{had} and Γ_{lep}. Here Γ^0_{had} stands for the hadronic width without QCD corrections ($\alpha_s = 0$). The error of ± 0.03 corresponds to a variation of m_t between 90 and 200 GeV and m_H in the range 50-1000 GeV. Instead of R_Z also the ratio of the peak cross sections

$$R \equiv \sigma^{\text{peak}}_{\text{had}} / \sigma^{\text{peak}}_{\text{lep}} = 19.77 \cdot (1 + \delta_{\text{QCD}})$$

can be used to derive α_s [25]. The quantity R can be measured directly, without need for off-peak data, knowledge of luminosity or line shape fitting.

The QCD correction can be cast in the form [26]

$$\delta_{\text{QCD}} = 1.05 \cdot \frac{\alpha_s}{\pi} + 0.9 \cdot (\frac{\alpha_s}{\pi})^2 - 13 \cdot (\frac{\alpha_s}{\pi})^3 \, ,$$

where the recently calculated third order correction [23] and charm and bottom mass effects and the top mass dependence [27] are taken into account.

Figure 9 summarizes recent LEP measurements of R_Z [28, 29, 30, 31].

From the average value

$$R_Z = 20.92 \pm 0.11$$

one gets

$$\boxed{\alpha_s(M_Z) = 0.141 \pm 0.017} \, ,$$

where the error is completely dominated by experimental (statistical) uncertainties[1]. The effect of the third order correction is small: leaving it out changes α_s to 0.137.

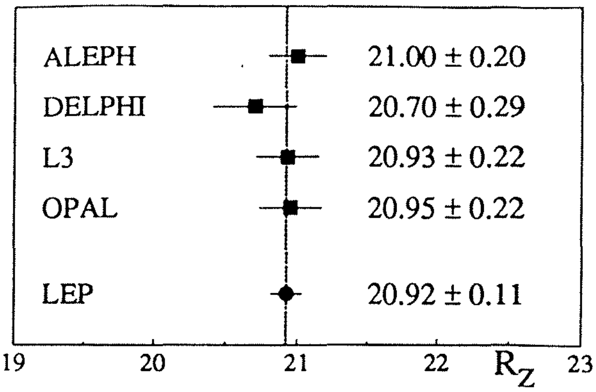

Figure 9: Measured values for $R_Z = \Gamma_{\text{had}}/\Gamma_{\text{lep}}$.

Also the total width of the Z^0 is in principle a measure of the QCD correction δ_{QCD}. However, Γ_{tot} depends strongly on the top quark mass. From a combined fit of all LEP cross section and asymmetry data one can determine m_t and α_s simultaneously, leading to a value of the strong coupling constant consistent with the number given here, but with slightly reduced errors [32].

4.3. Measurements of α_s from event topology

Many variables can be analyzed to determine α_s from the topology of hadronic events. As an example of a QCD analysis at LEP the measurement of α_s from jet rates by L3 [33] will be described briefly.

Jets can be defined by using an invariant mass jet algorithm. Most frequently the JADE jet finder [34] is used: For each pair of particles i and j the scaled invariant mass squared

$$y_{ij} = 2 \, \frac{E_i E_j}{E^2_{\text{vis}}} \, (1 - \cos\theta_{ij})$$

is evaluated. E_i and E_j are the particle energies and θ_{ij} is the angle between particles i and j. $E_{\text{vis}} = \sum_i E_i$ denotes the total energy of the event. The pair for which y_{ij} is smallest is replaced by a pseudoparticle k with four-momentum

$$p_k = p_i + p_j \, .$$

[1] In ref. [24] the possible effect of coherence of $u\bar{u}$ and $d\bar{d}$ final states on the Z^0 hadronic decay width has been estimated to be of the order of $+5 \pm 5$ MeV. Taking this correction into account would change the value of α_s from 0.141 ± 0.017 to 0.133 ± 0.018.

This procedure is repeated until all y_{ij} exceed the jet resolution parameter $y_{\rm cut}$. The remaining (pseudo)particles are called jets. Increasing $y_{\rm cut}$ lowers the fraction of multijet events but increases the separation of the jets. In this recombination scheme there is a close agreement between jet rates on parton and detector level.

Other invariant mass jet algorithms (E, E_0, p...) can be defined using slightly different expressions for y_{ij} and p_k [15, 35]. The JADE scheme is equivalent to the E_0 scheme for 4 massless partons with respect to jet counting.

The L3 analysis is based on 37,000 hadronic Z^0 decays at a center of mass energy of 91.2 GeV. Charged and neutral particles are measured in the electromagnetic detector and the hadron calorimeter which covers the polar angular range $|\cos\theta| < 0.996$. The jet rates obtained with the JADE algorithm are corrected for detector effects, resolution and acceptance, and also for initial state photon radiation. All these corrections are smaller than 10%.
The measured jet fractions are compared to the analytical 2$^{\rm nd}$ order QCD calculation for the E_0 scheme [15, 9]. A small $y_{\rm cut}$ dependent hadronization correction of 1–5 % is applied.

From the measured 3-jet fraction at $y_{\rm cut} = 0.08$,

$$f_3 = 18.4\,\% \pm 0.9\,\% \,,$$

and the central value of the renormalization scale $\mu^2/s = y_{\rm cut} = 0.08$ [36], the strong coupling constant is determined to be:

$$\alpha_s\,(M_Z) = 0.115 \pm 0.005\,(\mathrm{exp.})\,^{+0.012}_{-0.010}\,(\mathrm{theor.})\,.$$

The theoretical error is dominated by unknown higher order corrections, which have been estimated from a variation of the renormalization scale μ in the range 3 GeV – 91 GeV [37].

The relation between unknown higher order corrections and renormalization scale uncertainties shall be explained briefly: The scale dependence of the 3-jet fraction in 2$^{\rm nd}$ order is given by

$$f_3(\mu^2) = A\cdot\alpha_s(\mu^2) + (A\cdot b_0\cdot\ln(\mu^2/s) + B)\cdot\alpha_s^2(\mu^2)\,.$$

Here A and B denote the first and second order coefficients as calculated in [38, 15]. While α_s rises with decreasing μ (for fixed QCD parameter Λ), the term proportional to $\ln(\mu^2/s)$ becomes smaller. The renormalization scale is not predicted in QCD, however different recipes have been suggested for the choice of μ [39, 37, 40, 36]. They lead to values in the range 3 to 91 GeV for $\sqrt{s} = M_Z$. The values of $\Lambda_{\overline{MS}}$ and $\alpha_s(M_Z)$ determined from a comparison of data and QCD depend on the renormalization scale used in the above formula. If f_3 is calculated to *all orders*, an exact cancellation of the renormalization scale dependence appearing in α_s and in terms containing powers of $\ln(\mu^2/s)$ occurs, and the 3-jet rate becomes independent of the scale μ. Therefore the variation of $\alpha_s(M_Z)$ with μ is an estimate of uncalculated higher order corrections.

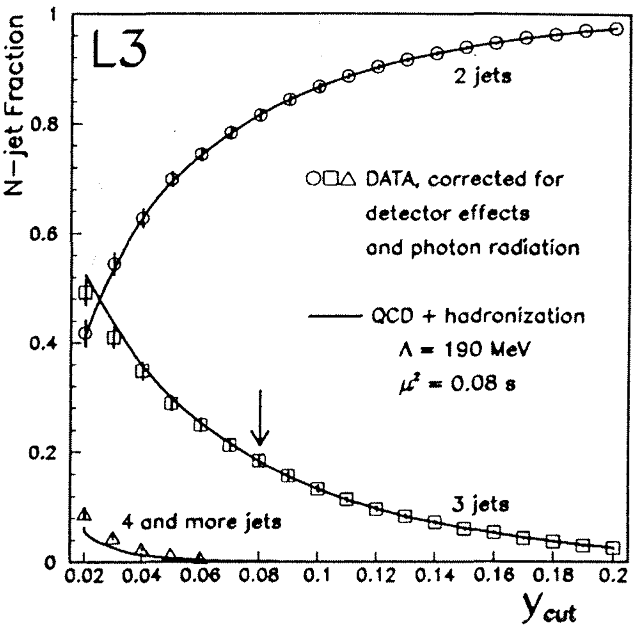

Figure 10: Jet fractions measured by L3

Figure 10 compares the measured jet fractions as a function of $y_{\rm cut}$ with the QCD predictions for $\alpha_s = 0.115$ (corresponding to $\Lambda = 190$ MeV) and $\mu^2 = 0.08 \cdot s$ [33]. The deviation in the jet rates at low values of $y_{\rm cut}$ is due to higher order corrections which are not yet calculated [41].

Similar results on jet fractions and α_s have been obtained by ALEPH [42], DELPHI [43], OPAL [35] and MARK II [44].

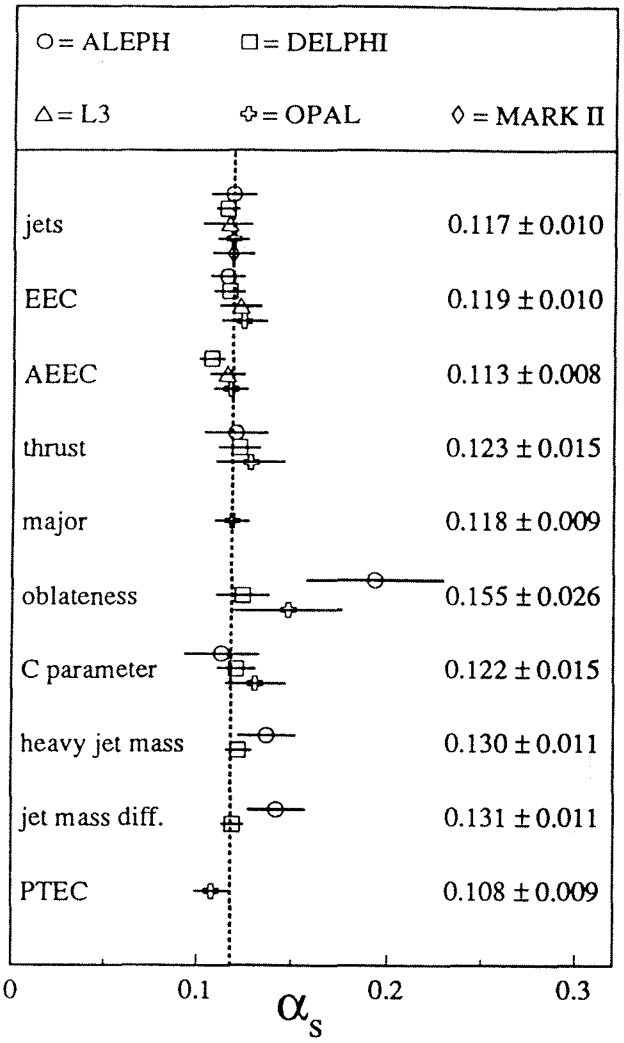

Figure 11: α_s from event topology

Values for α_s have been derived also from the study of energy-energy correlations (EEC) and its asymmetry (AEEC) and from distributions of global event shape variables like thrust, C parameter, etc. [15, and references therein]. All those results obtained by the five experiments ALPEH [42, 45], DELPHI [43, 46, 47], L3 [33, 18], OPAL [35, 48, 49, 50, 51] and MARK II [44] are summarized in figure 11.

The combination of all these numbers into one global LEP α_s value is difficult for two reasons: (1) The errors are dominated by theoretical uncertainties, which can only be estimated, (2) α_s numbers derived from the various quantities are correlated.

Therefore, in order to derive a combined value, first the experimental and theoretical uncertainties need to be estimated.

As an example for the agreement between different measurements figure 12 compares the 3-jet fractions for a jet resolution parameter of $y_{\rm cut} = 0.08$ as measured by the four LEP experiments [42, 43, 33, 35]. The weighted average has a relative error of about 1.5%.

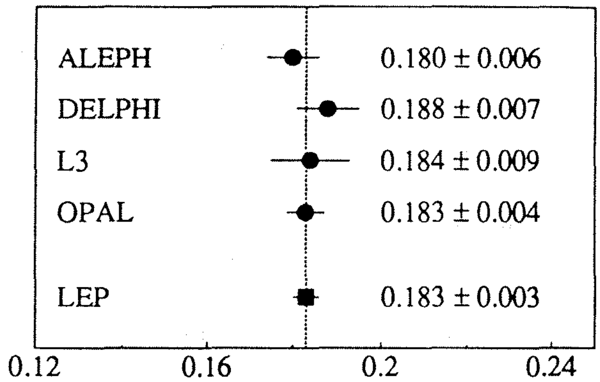

Figure 12: 3-jet fraction

A similar comparison of experimental results is shown in figure 13 for the integral of the asymmetry of energy energy correlations between 36° and 90° [46, 18, 48]. Also in this case the different measurements agree. The accuracy of the weighted average is 2.5% in this case.

Also for the other event shape variables sensitive to the strong coupling constant the different LEP measurements are consistent with each other. The *experimental precision* is variable-dependent. The relative experimental accuracy of the combined LEP results for α_s can be conservatively estimated to be $\approx 3\%$.

The *theoretical uncertainties* for α_s from event topology are due to (a) missing higher order (> 2) corrections in the perturbative expansion, and (b) hadronization.

Theoretical uncertainties of type (a) turn out to be the dominant ones. They can be estimated in several ways [52]:

- Variation of the strong coupling constant with renormalization scale, see above.
- Analysis of spread of α_s values for different variables.
- Study of effects of higher orders in parton shower Monte Carlo generators.

The three methods lead to similar numerical estimates of 5% - 10% for the theoretical uncertainties due to uncalculated higher order corrections.

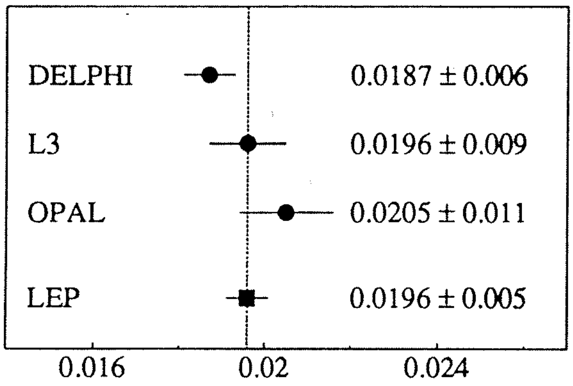

Figure 13: AEEC, integral between 36° and 90°

In this context it is interesting to study if the series expansion in α_s exhibits convergence: The OPAL data [19] have been used to derive α_s in first and second order from five event shape variables [51]. While the lowest order results scatter between 0.007 and 0.205, the agreement becomes much better when next to leading corrections are included (0.098–0.142). This indicates the convergence of the series expansion.

Hadronization errors (b) can be estimated by

- variation of fragmentation parameters of a given fragmentation model,
- change of model (see section 3).

For 'good' variables (like the 3-jet-fraction) the uncertainty is found to be of the order of 3%.

To compute a global value for α_s from event topology analyses two alternative recipes can be applied:

(i) First average α_s values derived from jet-fractions, energy correlations etc. over experiments, then combine results from the different variables.

(ii) First calculate combined α_s value for single experiment, then derive LEP average.

Method (ii), which will be applied here, has the advantage that correlations can be taken into account better. In addition, due to the smallness of the experimental errors, a comparison of the different LEP values of α_s and corresponding error estimates is effectively a comparison of the different analysis methods applied by the four LEP collaborations. Method (i) has been used previously, for example in ref. [53, 52, 54], with results similar to those derived here.

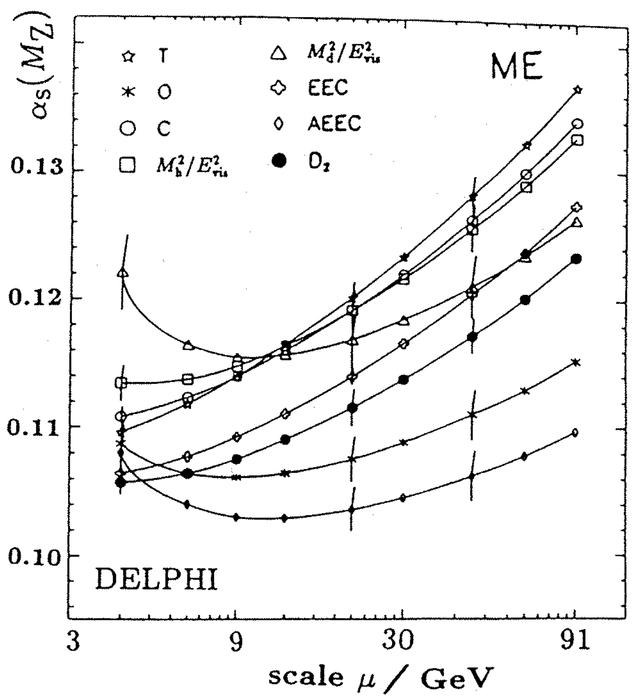

Figure 14: α_s values determined by DELPHI

As an example I will describe briefly results of the DELPHI α_s analysis [47], which is based on eight event shape variables, among them jet rates, thrust and energy-energy correlations. The measured distributions in these variables are corrected for detector effects and hadronization and then compared to the second order QCD calculations. To determine α_s, a fit is performed in a range of the shape variables where 3-jet contribution is dominant and where the corrections are small.

Figure 14 shows the values of $\alpha_s(M_Z)$ as function of the renormalization scale μ for the eight variables [47]. Indicated are some typical experimental errors. The difference in α_s values obtained from the different quantities as well as the μ dependence indicate that higher order effects are not negligible. For small scales μ the spread of the α_s values is substantially reduced, indicating that only the region of small renormalization scales should be considered. The average α_s value corresponding to figure 14 is found to be $\alpha_s = 0.109 \pm 0.002\,(\mathrm{exp})^{+0.007}_{-0.006}\,(\mathrm{theor})$. Here correlations between the variables are taken into account. The theoretical error is estimated from the spread of α_s values as function of shape variable and renormalization scale. Also hadronization uncertainties are included.

The whole analysis is performed twice. Once the QCD prediction is calculated using the ERT matrix element (ME) [9] option in JETSET and string fragmentation with parameters tuned for this case. The results are shown in figure 14. In a second analysis the hadronization correction is calculated using the parton shower option in JETSET. In this case the parton level distributions as calculated numerically in ref. [15] are used. The second method leads to a slightly higher average α_s value. Combining the results of the two methods gives finally for the strong coupling constant from event topology

$$\alpha_s(M_Z) = 0.111^{+0.007}_{-0.006}\,.$$

Also the other LEP experiments have derived an 'average' or 'best' value for α_s and an estimate of the uncertainty. The results are shown in figure 15.

The ALEPH value [45] is obtained from a combined analysis of energy-energy correlations and the global event shape variables thrust, C-parameter and oblateness for pre-clustered events.

L3 has measured the strong coupling constant from jet rates [33], energy-energy correlations and its asymmetry [18]. The value given in figure 15 is that from the AEEC analysis. This one has a slightly smaller error than the other two α_s values, which are consistent with the former one.

The OPAL number for the strong coupling constant in figure 15 is an average of α_s values [55] as measured from jet rates [35], energy correlations and asymmetry [48], planar triple energy correlations [49] and global event shape variables [50].

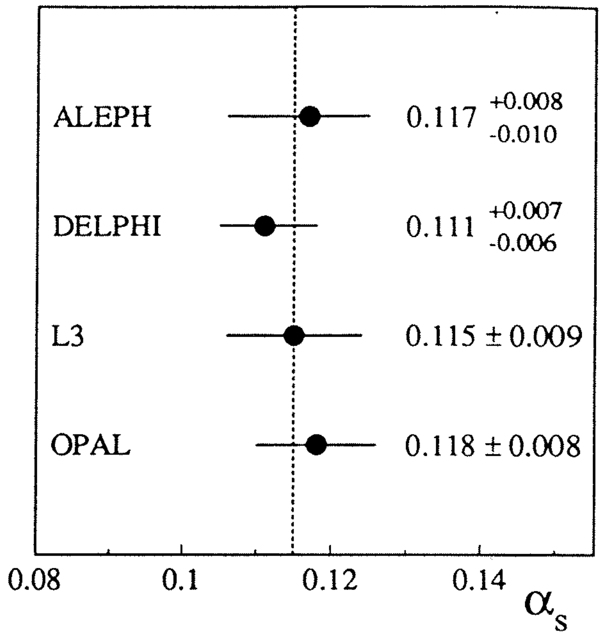

Figure 15: α_s values from event topology

The numbers and also the error estimates in figure 15 are consistent with each other. Since the errors are dominated by theoretical uncertainties, which are common to all four numbers, I combine the results of the figure by calculating the unweighted means, both for the central value and the error. The final result for the α_s value measured from the event structure at LEP becomes

$$\boxed{\alpha_s(M_Z) = 0.115 \pm 0.008}\,.$$

4.4. Comparison and summary of α_s results

Figure 16 compares the α_s values obtained from R_Z and from the event shape. It has to be stressed that these two determinations are independent and that in one case (R_Z) the error is dominated by experimental uncertainties, while in the other case (event shape) the theoretical error is largest.

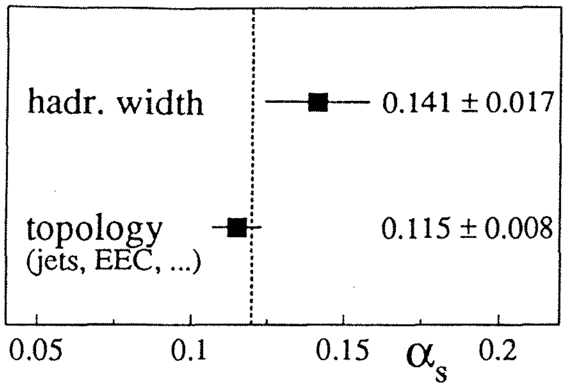

Figure 16: Summary of α_s values measured at LEP

The weighted mean value of

$$\boxed{\alpha_s = 0.120 \pm 0.007}$$

is dominated by the α_s determination from the event topology. This corresponds to [22]

$$\Lambda^{(5)}_{\overline{\rm MS}} = 250^{+110}_{-\ 80}\ \mathrm{MeV}\ .$$

With a relative accuracy of about 6% the α_s measurement at LEP is one of the most precise determinations of the strong coupling strength, see following subsection. It has to be underlined that this error includes *all* theoretical uncertainties; there is no additional model dependence.

4.5. α_s values from different processes

A comparison of α_s values obtained in various processes such as deep inelastic lepton-nucleon scattering, $p\bar{p}$ collisions and e^+e^- annihilation constitutes an important test of the universality of QCD. Figure 17 shows such a comparison. Only those processes are taken into account, which allow for relatively precise determinations of α_s. All measurements of the strong coupling strength have been translated into $\alpha_s(M_Z)$. These numbers are in good agreement with each other.

The α_s value from τ decays is obtained from semileptonic branching ratios measured by the L3 collaboration [56]. The numbers for Υ decays, photon structure function and from e^+e^- event topology at 35 GeV are taken from ref. [57]. The strong coupling constant shown in figure 17 for deep inelastic scattering is an unweighted average of two recent analyses [58, 59]. The sixth number in the figure is derived from measurements of W + jet production in $p\bar{p}$ collisions by UA2 and UA1 [60]. Measurements of R in e^+e^- annihilation have been combined and analyzed in ref. [61]. The value in figure 17 corresponds to data taken at center of mass energies around 35 GeV and is computed as the average value of the three α_s values given in [61]. Data at $\sqrt{s}$ values between 20 and 65 GeV are consistent with the 35 GeV result.

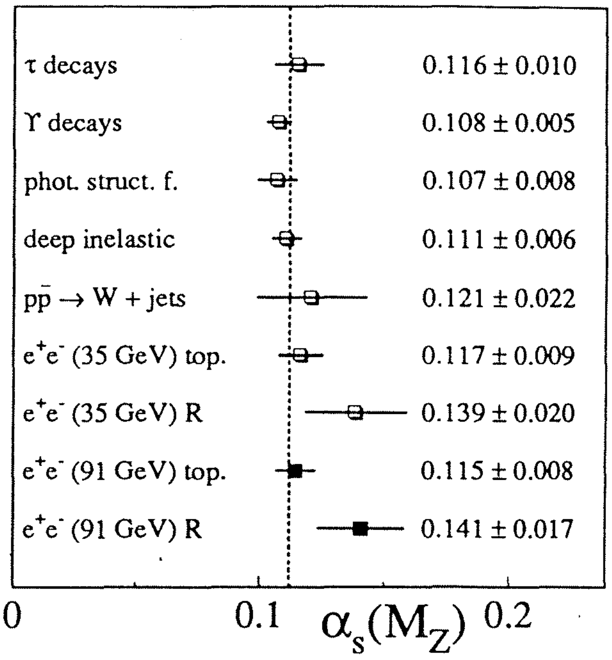

Figure 17: α_s values at the scale $\mu = M_Z$

The meaning of the errors shown in figure 17 is not the same for all α_s values, since often some uncertainties (such as scale dependence) are not included. Ignoring this warning and taking the weighted average of all numbers yields for the global average $\alpha_s = 0.113 \pm 0.003$ and $\chi^2/N_{\rm Dof} = 6.5/8$.

The e^+e^- values, in particular from R, are somewhat high, but still consistent with the other results. Future improvements in accuracy at LEP will reveal if there is a discrepancy or not.

Since the various measurements involve different quark flavors and different energy scales, a comparison of the α_s values is also a test of flavor independence and running.

4.6. Flavor independence of strong interactions

The L3 collaboration has presented a study of the strong coupling constant for bottom quarks [62, 63].

At the Z^0 pole the fraction of bottom events in the hadron sample is 22%. The b-quark content can be enhanced by selecting hadronic events with muons or electrons from semileptonic decays of heavy B mesons or hadrons. In a hadron sample of 110,000 events L3 finds 1,800(1,100) events with muons(electrons) of momenta above 4(3) GeV and $p_\perp$ with respect to the nearest jet exceeding 1.5(1.0) GeV. In the inclusive lepton subsample 87% of the events contain bottom quarks.

For both samples the 3-jet rates are measured as described in subsection 4.3. One gets for the ratio of 3-jet rates at $y_{\rm cut} = 0.05$, after corrections for detector, hadronization and bottom mass effects:

$$\frac{f_3^{\mu,e}}{f_3^{had}} = 1.00 \pm 0.03\,({\rm stat}) \pm 0.04\,({\rm syst})\ .$$

With the known bottom content in the two data sets of $22 \pm 0.5\%$ and $87 \pm 3\%$ one can calculate the ratio of α_s values for b quarks and the lighter species:

$$\alpha_s^{\rm b}/\alpha_s^{\rm udsc} = 1.00 \pm 0.08\ .$$

Here the quarks u,d,s,c are assumed to have the same coupling strength. This result agrees with the QCD expectation of one. The precision is significantly better than that achieved previously [64, 65].

From a comparison of jet rates at the Z^0 resonance and at lower center of mass energies one can derive [52]

$$\alpha_s^{\rm uc}/\alpha_s^{\rm dsb} = 0.96 \pm 0.10\ ,$$

which confirms the independence of the strong coupling of the electric charge.

4.7. Running of α_s

Figure 18 shows the 3-jet fraction for $y_{\rm cut} = 0.08$ measured in e^+e^- annihilation for center of mass energies between 14 and 60 GeV [34, 66] and at 91 GeV [42, 43, 33, 35]. In leading order the 3-jet rate is proportional to the strong coupling constant α_s.

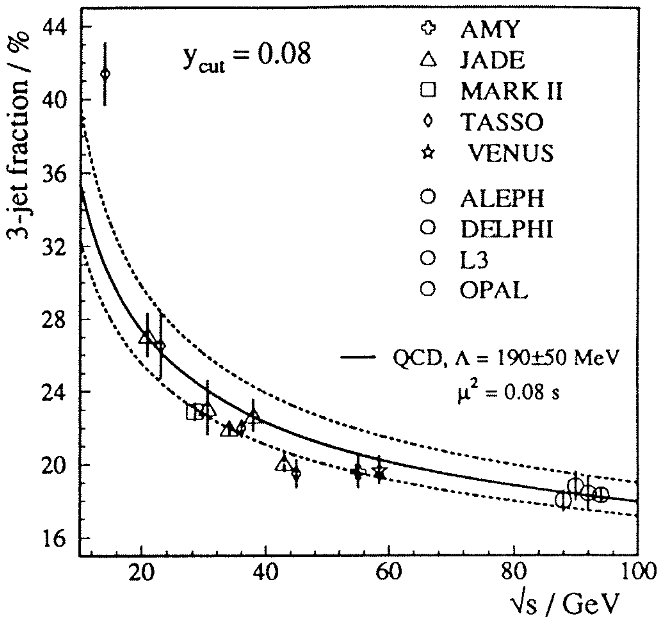

Figure 18: Energy dependence of the 3-jet fraction

The energy dependence is reproduced by QCD. The value $\alpha_s = 0.115$, corresponding to the averaged jet fractions measured at LEP, and $\mu^2/s = y_{\rm cut} = 0.08$ are used for the QCD prediction, which is corrected for hadronization effects. An energy independent strong coupling constant can be ruled out from the comparison of all measured 3-jet fractions.

The set of experimental results shown in figure 18 demonstrates unambiguously the running of α_s and provides indirect evidence for the gluon self coupling. This is a very important confirmation of QCD.

The running of α_s can also be demonstrated using values derived from the analysis of the asymmetry of energy-energy correlations [18].

5. Test of QCD matrix element

With the only free parameter in QCD, α_s, known, the QCD matrix element calculations can be tested by comparing the measured jet distributions in multi-jet events to the theoretical predictions. Events with 3 jets can be used to distinguish between QCD with spin-1 gluons and an alternative model with scalar gluons. The triple gluon vertex contributes to events of type $e^+e^- \to q\bar{q}gg$. Thus 4-jet events can be used to distinguish between QCD and an abelian model without boson self coupling.

In the case of 3-jet events the QCD calculations are available in next to leading order, while the distributions for 4-jet final states have been calculated only on the Born level so far.

5.1. 3-jet events

For unpolarized beams, an event of type $e^+e^- \to$ 3 jets can be described by four independent kinematical variables (apart from the jet masses).

They can be chosen as

- x_2 = energy of the second most energetic jet normalized to the beam energy
- x_3 = energy of the least energetic jet normalized to the beam energy
- $\bar{\theta}$ = polar angle of the normal to the event plane with respect to the e^- direction
- χ = angle between the jet plane and a plane spanned by the first jet and the beam

Here no distinction between quark, antiquark and gluon jets is made. I refer to the most energetic jet as the 'first jet', i.e.: $x_1 > x_2 > x_3$ and $x_1 + x_2 + x_3 = 2$.

The distributions in those four variables are sensitive to the gluon spin (0 or 1).

The jet energy distributions have been measured by L3 [67] and OPAL [68], the event orientation has been studied by DELPHI [69] and L3 [67]. As examples two of those distributions are shown here [63].

Figure 19 shows the x_3 distribution obtained by L3 based on 20,800 3-jet events with transition values y_{23}, for which a 3-jet configuration turns into a 2-jet event, in the range $0.02 \leq y_{23} \leq 0.05$. The measurements are compared to the predictions of second order QCD [9] and of the scalar gluon model [70].

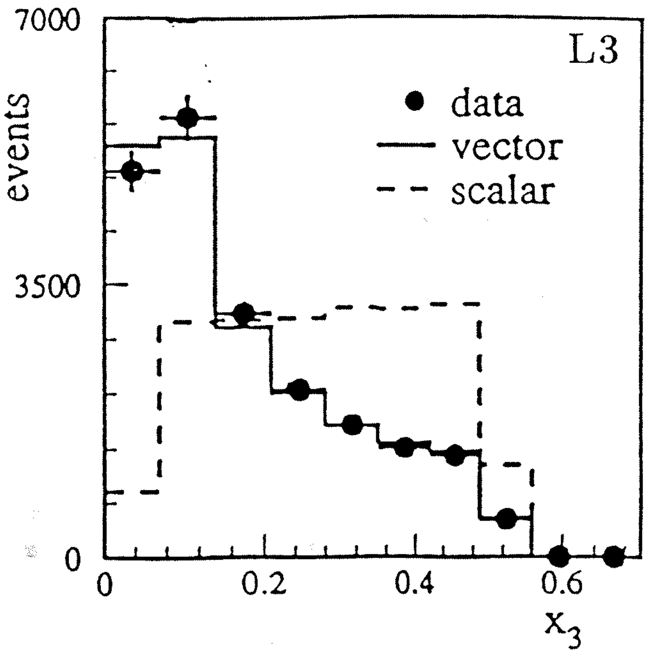

Figure 19: Distributions of x_3 measured by L3

The distribution of the polar angle $\bar{\theta}$ has the form

$$\frac{d\sigma}{d\cos\bar{\theta}} \propto 1 + \bar{\alpha}(T) \cdot \cos^2\bar{\theta}$$

The value of the coefficient $\bar{\alpha}$ has been measured by DELPHI as function of the event thrust value, as shown in figure 20. The distribution is compared to the QCD prediction of $-1/3$ and the scalar model curve [71].

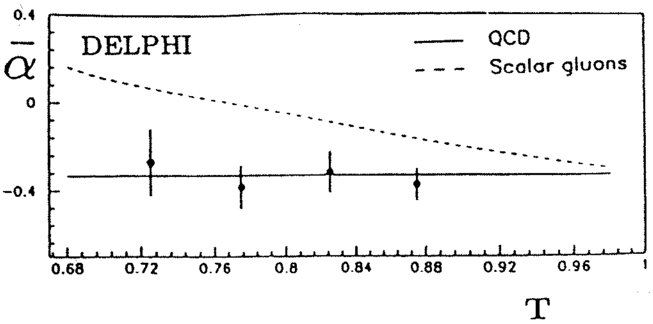

Figure 20: Distributions of $\bar{\alpha}$ measured by DELPHI

zero with a significance of more than five standard deviations[2]. The abelian model can be ruled out both from the measured ratios N_C/C_F and T_F/C_F. QCD reproduces the data very nicely. A distinction between SU(2), SU(3) and SU(4) is not yet possible.

	N_C/C_F $g \to gg$	T_F/C_F $g \to q\bar{q}$
LEP	2.0 ± 0.3	0.3 ± 0.2
QCD	2.25	0.375
abelian	0	3

Table 3: Color factor ratios

LEP has provided clear evidence for the existence of the triple gluon vertex and has found the coupling strength to be in quantitative agreement with the QCD predictions. Thus one of the fundamental properties of the gauge theory of strong interactions has been tested.

Also in the electroweak Standard Model with an SU(2)xU(1) gauge structure boson self coupling is expected to exist. However, this theoretical prediction could not yet be tested directly since the W bosons are so heavy. Only when LEP will take data at center of mass energies above the W pair production threshold, in a few years from now, the self interactions of the bosons γ, W and Z can be studied experimentally.

[2]In the ALEPH and DELPHI analyses higher order corrections to the shape of the 4-jet distributions are assumed to be small; this is motivated by the smallness of the second order corrections to the form of the 3-jet distributions.

6. 'Soft' hadron physics

In the preceding sections measurements and QCD predictions have been compared at the *jet level*, corresponding to 'hard' quarks and gluons.

In this section hadronic events are investigated at the *hadron level* and measurements of particle spectra, string effect, local particle density fluctuations etc. are presented. For many 'soft' phenomena QCD predictions exist, in form of parton shower Monte Carlo generators and analytical (next to) leading log calculations. However, in studies at the hadron level the importance of fragmentation and particle decays is significantly increased with respect to the jet-level analyses. Consequently it is difficult to test the perturbatively calculated QCD predictions and the hadronization schemes separately.

First I will outline briefly the qualitative results of the QCD calculations for particle spectra, string effect etc. Then I will describe the various measurements done at LEP and compare the results to the QCD predictions.

6.1. Gluon interference

Interference of gluons leads to the following two phenomena:

- INTRA-jet effects

  The (next to) leading log QCD calculations [86, 87] take into account interference effects between soft gluons, as prescribed by Quantum Mechanics. In this context the expression 'soft gluon coherence' is frequently used. One finds that *destructive* interference occurs if the emission angles in subsequent parton branchings increase. This means that effectively the subsequent angles decrease, as shown schematically in figure 24 [87]. This phenomenon is generally referred to as 'angular ordering' and used for example in parton shower generators to take into account interference effects.

  Consequently the available phase space for soft gluons inside a jet is decreased. This leads to reduced parton multiplicities and a suppression of partons with low momentum.

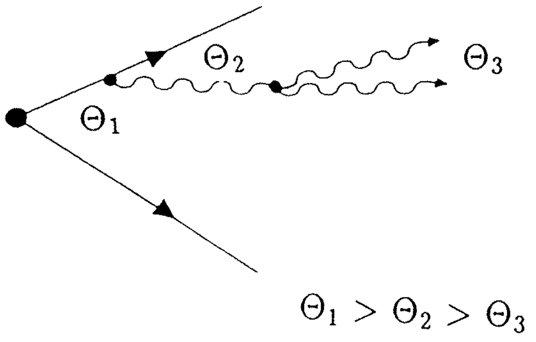

Figure 24: Angular ordering

- INTER-jet effects

  Analytical QCD calculations predict for 3-jet events destructive inter-jet interference effects in the region between the q and the $\bar{q}$ jets [88, 87]. Thus less particles are produced in between the quark and antiquark jets in comparison to the other two inter-jet regions. This is known as the 'string effect', see below.

To be able to test the parton level predictions a model for hadronization and decays is needed. In case of Monte Carlo generators string or cluster fragmentation is used together with empirical decay tables. In the context of analytical calculations the hypothesis of 'Local Parton Hadron Duality' (LPHD) [89, 90] is invoked. It suggests that the calculated parton distributions can be compared directly to the measurements for (long lived) hadrons.

6.2. Charged particle multiplicity

All five experiments have measured the charged particle multiplicity distributions and compared their results to different models [91, 92, 93, 20, 19]. The parton shower Monte Carlo programs can reproduce the data well. This is also true for the log-normal probability function [94] and, to a lesser extent, for the negative binomial distribution, as shown in figure 25 for the ALEPH analysis [91]. Next to leading order QCD calculations [95, 96] can reproduce the width of the multiplicity distribution within 10% [91].

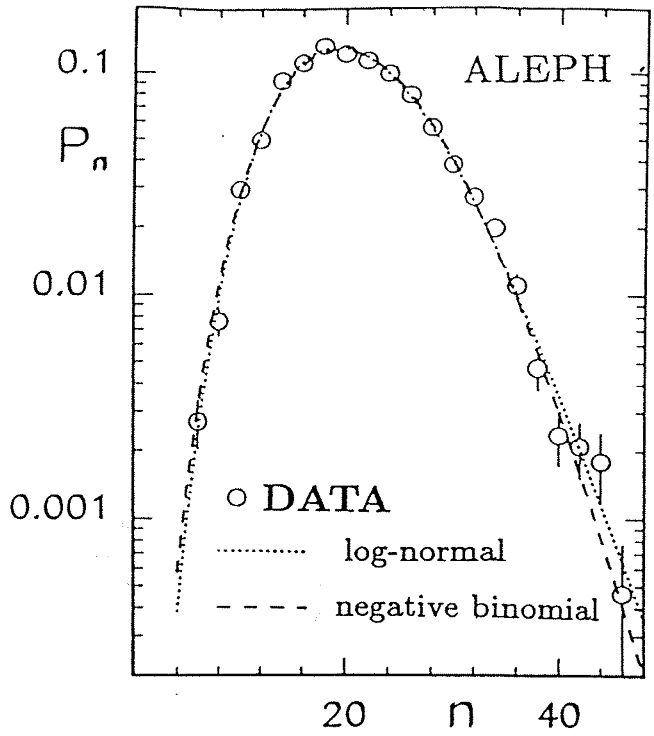

Figure 25: Charged particle multiplicity distribution from ALEPH

A comparison with lower energy e^+e^- data supports the KNO scaling hypothesis [97], that the distribution of $n/\langle n\rangle$ is independent of the center of mass energy.

More detailed studies have been performed by DELPHI [98]. The dependence of the multiplicity distribution on rapidity, jet configuration and transverse momenta has been measured [92, 99]. In all cases good agreement between data and the JETSET Monte Carlo has been found.

The values for the average charged multiplicity are shown in figure 26. All the primary produced particles or those produced in the decay of particles with an average lifetime smaller than 10^{-9} s are considered.

The weighted average of

$$\langle n_{\mathrm{ch}}\rangle = 20.8 \pm 0.2$$

is in agreement with the predictions made by the JETSET and HERWIG generators.

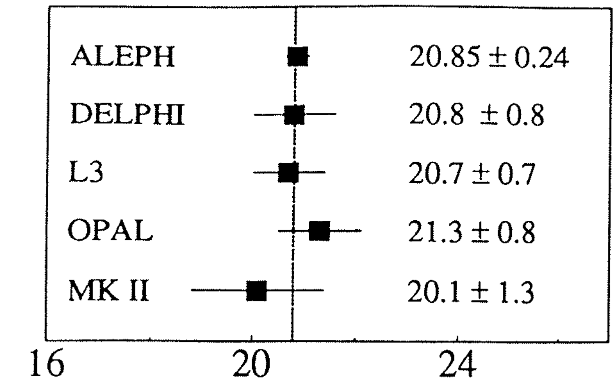

Figure 26: Mean charged multiplicity

Figure 27 shows the increase of $\langle n_{ch} \rangle$ with center of mass energy between $\sqrt{s} = 14$ and 91 GeV.

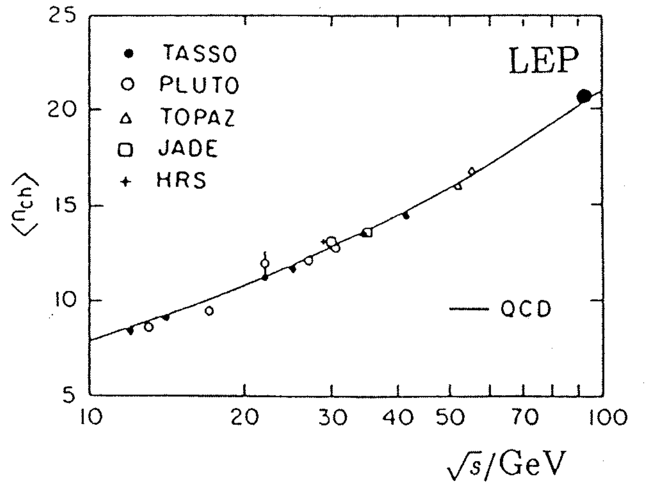

Figure 27: Charged multiplicity as function of center of mass energy

The energy dependence can be reproduced by an analytical QCD calculation (plus LPHD), which predicts a function of the form [100]

$$\langle n \rangle = a \cdot (\alpha_s(s))^{\beta} \cdot \exp(\gamma / \sqrt{\alpha_s(s)}) \, .$$

The parameters β and γ are predicted as a function of the number of flavors n_f, while the normalization factor a can not be calculated. The QCD fit shown in figure 27 [15], which describes all measurements well, has been made considering only the data below the Z^0 peak. As can be seen the QCD curve predicts correctly the average charged multiplicity at 91 GeV.

This is a first success of the analytical QCD calculations.

6.3. Particle identification (light flavors)

Before discussing particle spectra for different hadrons I will briefly describe how light hadrons (those made out of u, d and s quarks) are identified in hadronic Z^0 events.

Figure 28 shows the $\gamma\gamma$ invariant mass distribution as measured by L3 [93].

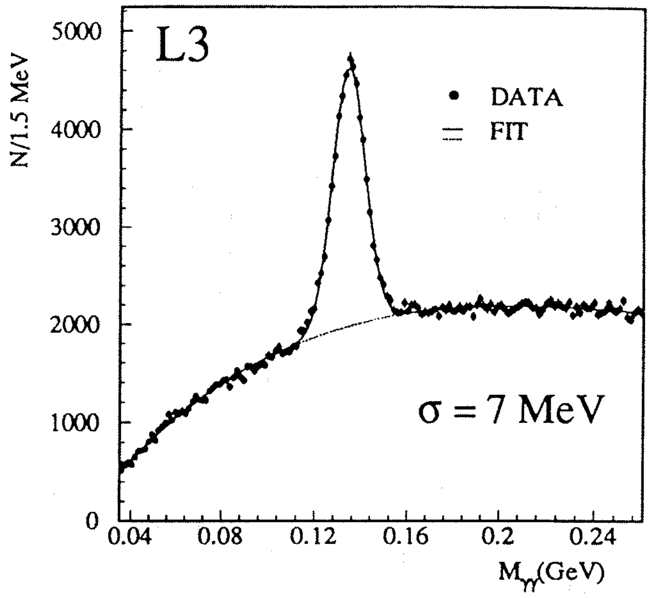

Figure 28: $\gamma\gamma$ invariant mass distribution measured by L3

The peak position coincides with the neutral pion mass of 135 MeV. It has a width of about 7 MeV and contains 31,000 π^0 mesons. This analysis is based on isolated photons measured in the electromagnetic calorimeter. The π^0 detection efficiency varies between 2% and 6% depending on the meson momentum.

Short lived neutral kaons have been identified by OPAL [101] and DELPHI [102], using similar analysis techniques: K^0_s mesons ($m = 498$ MeV, $c\tau = 2.7$ cm) are reconstructed from pairs of oppositely charged particles (assumed to be pions) originating from a secondary vertex. The resulting invariant mass spectrum is shown in figure 29 for the OPAL analysis [101].

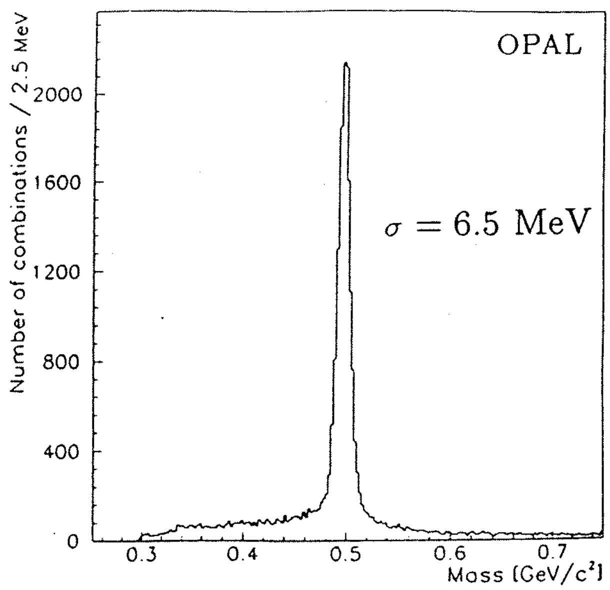

Figure 29: $\pi^+\pi^-$ invariant mass distribution measured by OPAL

This analysis is based on the information from the central tracking chambers. The peak contains 14,000 kaons and has a width of 6.5 MeV. The reconstruction efficiency varies between 5% and 27%, depending on the K^0_s momentum.

The production of charged kaons with momenta between 1 and 2 GeV has been measured by DELPHI using the barrel RICH (Ring Image CHerenkov counter) [102]. The yield is found to agree with that of neutral kaons.

DELPHI has also identified $K^{*\pm}$ mesons (892 MeV) [102] via the decay chain

$$K^{*\pm} \rightarrow K^0_s + \pi^\pm \rightarrow \pi^+\pi^- + \pi^\pm .$$

Baryons in form of Λ's ($m = 1116$ MeV, $c\tau = 7.9$ cm) have been reconstructed by DELPHI [103]. Hadrons are measured in the central tracking detectors. Pairs of oppositely charged particles originating from a secondary vertex are selected. One of the particles is assumed to be a proton, the other a pion. The resulting invariant mass spectrum is shown in figure 30 [103]. The width of the distribution is about 4 MeV.

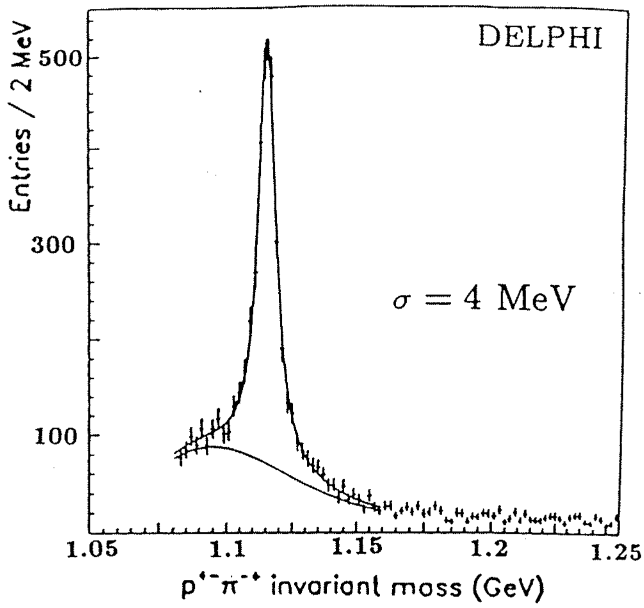

Figure 30: $p\pi$ invariant mass distribution measured by DELPHI

The average number of mesons and baryons per hadronic Z^0 decay is shown in table 4. The numbers are the sums of particle and antiparticle yields. In case of the neutral kaons both K^0_s and K^0_l are included.

hadron	$\langle n \rangle$	reference
π^0	9.8 ± 0.7	[93]
K^0	2.04 ± 0.10	[102, 101]
$K^{*\pm}$	0.93 ± 0.25	[102]
Λ	0.25 ± 0.03	[103]

Table 4: Particle yields in hadronic Z^0 decays

The particle yields normalized to the average charged multiplicity are in agreement with the measurements at lower center of mass energies [104].

6.4. Particle spectra

An interesting prediction of perturbative QCD concerning the inclusive momentum spectra is the reduction of the number of soft gluons due to destructive interference. This behavior can be studied best in terms of the variable $\xi_p = \ln 1/x_p$, where x_p denotes the ratio of particle momentum p to the beam energy $\sqrt{s}/2$. The QCD calculations predict a ξ_p distribution with a maximum, ξ_p^*, at ≈ 3.8 for $\sqrt{s} = 91$ GeV, which corresponds to $x_p \approx 0.02$ and $p \approx 1$ GeV [90, 105, 106, 107]. The value of ξ_p^* is predicted to move to higher values with increasing center of mass energy. For massive particles the spectrum is modified such that the peak position is shifted to lower values.

The result of QCD calculations in 'modified leading log approximation' (MLLA) [90, 87] can be written in the form:

$$\frac{1}{\sigma_{\text{had}}} \frac{d\sigma}{d\xi_p} = N(\sqrt{s}) \cdot f(\sqrt{s}, \Lambda_{\text{eff}}, Q_0; \xi_p)\,.$$

Here Λ_{eff} is an effective scale parameter, which is independent of center of mass energy and particle type. An increase in Λ_{eff} corresponds to a decrease in the position of the maximum, ξ_p^*. Q_0 is an effective cut-off parameter in the quark-gluon cascade and increases with particle mass. However, the exact relation between Q_0 and mass is not known. For light hadrons, such as pions, one can set $Q_0 = \Lambda_{\text{eff}}$ ('limiting spectrum'). The (unpredicted) normalization factor N, which describes the hadronization, is a function of the center of mass energy $\sqrt{s}$ and the particle type.

At the Z^0 resonance spectra have been measured [108] for neutral pions [93], Λ baryons [103], neutral kaons [102, 101] and also for all long lived charged particles [109, 93, 101]. Charged particles include, in addition to pions (80 %), heavier hadrons, mainly kaons (10 %) and protons (5 %), and have an 'average mass' of 220 MeV.

Figure 31 shows the measured ξ_p distributions for neutral pions [93], neutral kaons [101] and charged particles [110]. One sees clearly the 'humpbacked' shape of the distribution and a shift of the peak position to lower values with increasing particle mass.

Also the spectra predicted by QCD (MLLA) are shown, which describe the measured distributions fairly well, in particular in the region of the maximum. The QCD curves are obtained in the following way [111]: For all particles a value of $\Lambda_{\text{eff}} = 150$ MeV is used, for which all particle spectra can be described. In case of the the neutral pions the limiting spectrum ($Q_0 = \Lambda_{\text{eff}}$) is calculated, with an additional phase space factor $(p/E)^3$ [111]. For the kaons the ξ_p distribution is computed using $Q_0 = 300$ MeV, as determined from a comparison to the measured spectrum. In addition an estimate of the proton spectrum is shown, assuming an average number of protons per hadron event of about one [8]. Making use of isospin symmetry the QCD spectra for charged pions and kaons can be obtained from the calculated distributions for π^0 and K^0. Adding up the $\pi^{\pm}$, $K^{\pm}$ and p spectra gives the QCD prediction for the charged particles, shown by a dashed line in figure 31.

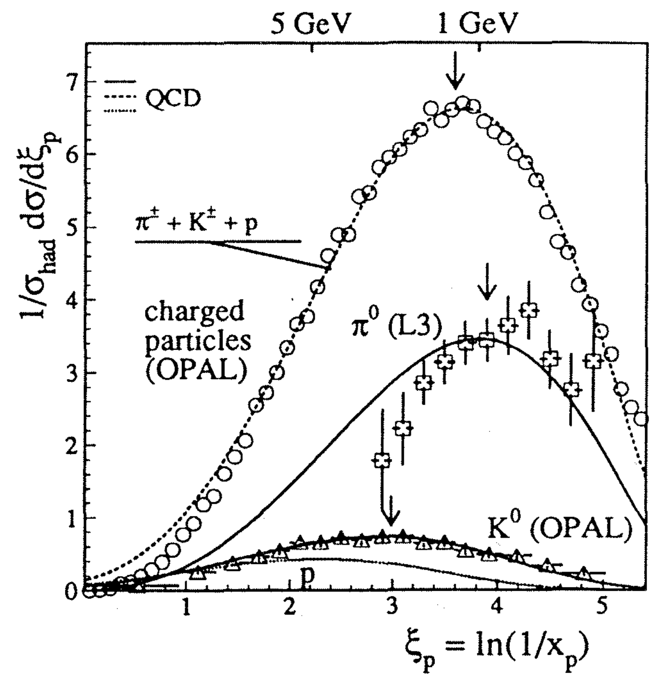

Figure 31: Measured ξ_p distributions for π^0, K^0 and charged particles in comparison with QCD predictions

Table 5 shows the measured peak positions as function of the particle mass. The result is in qualitative agreement with the QCD predictions. If one uses the limiting spectrum the measurements can be reproduced fairly well by setting Λ_{eff} equal to the particle mass given in table 5.

The OPAL collaboration has compared the measured ξ_p distribution also to the predictions of parton shower models with and without coherence effects [110]. Both can describe the data well, the differences are found to be small. It is even possible to reproduce the 91 GeV data with an incoherent parton shower plus independent jet fragmentation [112]. This analysis shows, that the suppression of low energy particles is not only due to soft gluon interference, but phase space effects.

hadron	m/MeV	ξ_p^*	reference
π^0	135	4.11 ± 0.18	[93]
charged	220	3.63 ± 0.02	[109, 93, 110]
K^0	498	2.91 ± 0.04	[102, 101]
Λ	1116	2.6 ± 0.4	[103]

Table 5: Peak position in ξ_p distribution

In order to distinguish between the two effects one can study the evolution of the position of the maximum with $\sqrt{s}$. Figure 32 shows the dependence of ξ_p^* for charged particles on the center of mass energy. For the data below the Z^0 resonance see [81] and references in [93].

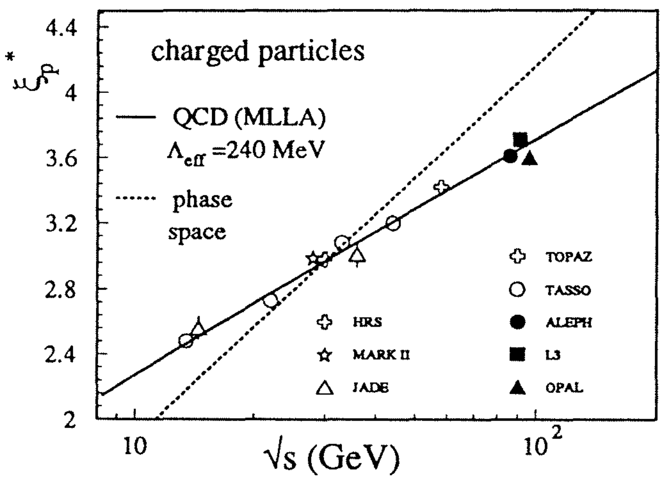

Figure 32: Position of the maximum in the ξ_p distributions for charged particles

Over the wide range from 9 to 91 GeV good agreement between data and QCD calculations is found, while the $\sqrt{s}$ dependence expected for phase space ($\xi_p = \ln\sqrt{s} +$ const) is clearly incompatible with the measurements. The same conclusion can be drawn from the center of mass energy dependence of ξ_p^* for neutral pions [93].

Both ALEPH and OPAL have also studied the center of mass energy dependence of ξ_p^* for parton shower models with and without gluon interference effects [109, 110]. The version of the JETSET program with coherent parton branchings describes the data as well as the MLLA curve. In the incoherent case the agreement is acceptable only if string fragmentation is used. This indicates that parton level interference effects can be effectively parametrized by the string model.

The above studies can be summarized in the following way:
Analytical (next to) leading log QCD calculations together with the simple LPHD assumption allow a quantitative description of particle spectra, and in particular of the center of mass evolution of spectra and average charged multiplicities.

6.5. *'String effect'*

After the studies of *intra*-jet coherence effects described in the last two subsections now *inter*-jet phenomena are to be analyzed.

About 10 years ago the JADE collaboration found that in events of type $e^+e^- \to 3$ jets at $\sqrt{s} \approx 30$ GeV less particles are produced in between the q and $\bar{q}$ jets in comparison to the other two inter-jet regions [113], see figure 33.

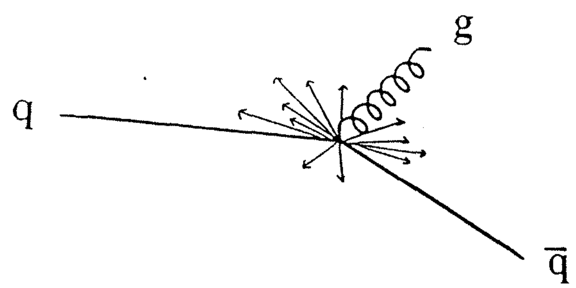

Figure 33: 'String effect'

The name 'string effect' was given to this phenomenon, a rather unfortunate choice because it does not distinguish between the observation and a possible interpretation.

This asymmetry in the particle flow in the 3-jet plane can be explained in different ways:
(a) String fragmentation [114]. In 3-jet events a string is stretched from the quark via the gluon

to the antiquark. Most particles are therefore produced in between the quark and gluon and in between the antiquark and the gluon, and only a few hadrons are created between the quark and antiquark.
(b) Analytical QCD calculations including coherence, predict destructive inter-jet interference effects in the region between the q and the $\bar{q}$ jets [88, 87].
(c) Differences in the parton shower evolution and/or fragmentation of the primary quarks and hard gluons.

While both models (a) and (b) describe qualitatively the string effect, they make different predictions for certain observables [88, 115, 116]. However, the corresponding measurements are difficult and have not been done yet.

The string effect can not be explained by models based on an incoherent parton shower plus 'independent jet fragmentation' [7, and references therein]. For this reason those hadronization schemes are hardly used any more.

Both DELPHI and OPAL have established, using different methods, the 'string effect' at 91 GeV [17, 117].

The DELPHI collaboration [17] has used a method similar to the one applied by JADE [113]. The 3 jets are energy ordered. The least energetic jet has a probability of more than 50% for being the 'gluon-jet'. Both parton shower models as well as the matrix element generator plus string fragmentation can reproduce the measured particle flow in the event plane, and in particular the asymmetry in the dips between jets 1,2 and 3,1. The matrix element generator together with an 'independent fragmentation model' can not describe the data.

The OPAL collaboration [117, 118, 119] has selected 3-jet events with at least one lepton. Most likely these are bottom or charm events. The lepton is required to be close to the second or third most energetic jet. The 'leptonless' jet out of the two least energetic jets is likely to be the gluon jet. In order to avoid kinematic biases only symmetric configurations are analyzed, for which the angle between the q and g jets is nearly the same as that between the q and $\bar{q}$ jets. For angles of $130° \pm 10°$ the purity of the 'gluon jet' is about 70%.

Figure 34 shows the measured particle flow in the event plane [117]. One curve (points) shows the particle flow starting at the high energy quark and ending at the gluon jet; the histogram is obtained by proceeding in the opposite sense. It can be seen clearly that there is a depletion of particles in between the most energetic quark jet and the second quark jet, compared to the region between the first quark and the gluon. This demonstration of the 'string effect' for heavy quark events does not involve any Monte Carlo comparisons and is therefore model independent.

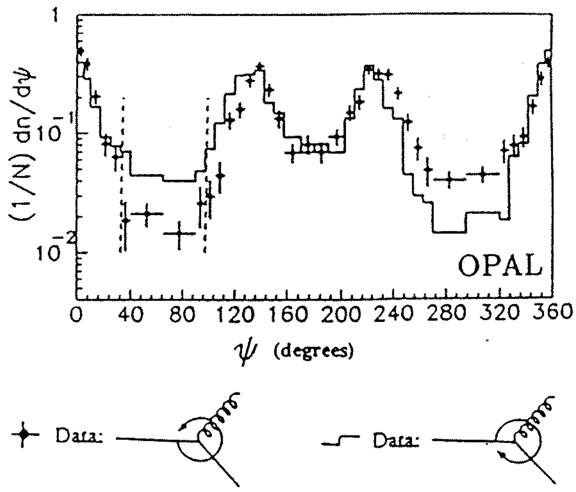

Figure 34: String effect measured by OPAL

In summary one can say that the 'string effect' is well established, but that a distinction between different possible interpretations is not yet possible.

To study inter-jet coherence effects further, an energy-multiplicity-multiplicity correlation function has been introduced in ref. [120]. It has been measured by ALEPH and DELPHI [109, 121]. Fair agreement between data and Monte Carlo calculations based on coherent parton showers and/or string fragmentation is observed. The correlation function obtained from the generator COJETS (incoherent parton shower plus independent jet fragmentation) [122] can not reproduce the data.

However, particle decays have a large influence on energy-multiplicity-multiplicity correlations [98], so that the interpretation of the measurements is difficult. Here more studies are needed.

6.6. Quark-jets versus gluon-jets

Gluons carry a larger color charge ($N_C = 3$) than quarks ($C_F = 4/3$). This leads to the qualitative QCD prediction that gluon jets are broader and contain softer particles than quark jets of the same energy.

OPAL has applied the quark tagging method as described in subsection 6.5 to study the difference between quark and gluon jets in a model independent way [118, 119]. The observed differences are rather small and can be summarized as follows:

- Gluon jets are broader than quark jets.
- Hadrons in the *core* of gluon jets ($\pm 15°$ around jet axis) are softer than in quark jets.
- Charged multiplicities are quite similar in quark and gluon jets.

The hadron spectra in quark and gluon jets are compared in figure 35 [118].

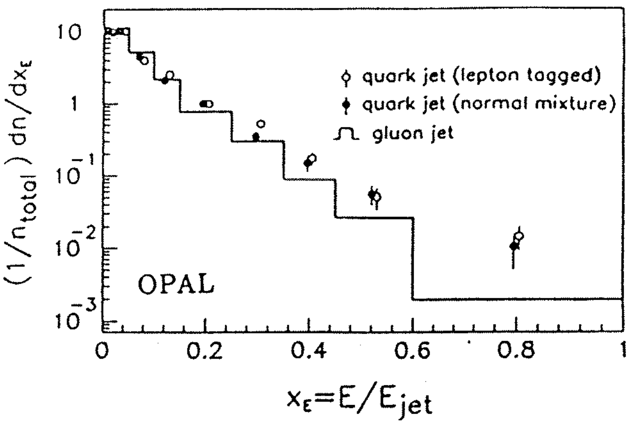

Figure 35: Hadron energy spectra in quark and gluon jets measured by OPAL

The charged multiplicities of quark and gluon jets have also been studied by DELPHI using a different method [99]: A sample of about 600 symmetric 3-jet events, in which all jets have nearly the same energy, is selected. If one orders the jets according to their multiplicities, $n_1 \geq n_2 \geq n_3$, the ratio $\langle n_1 \rangle / (\langle n_2 \rangle + \langle n_3 \rangle)$ is sensitive to the ratio of the average quark-jet and gluon-jet multiplicities. The measured value of $\langle n_{\text{gluon}} \rangle / \langle n_{\text{quark}} \rangle$ is consistent with unity.

The combined OPAL and DELPHI results on charged multiplicities in gluon and quark jets are

$$\langle n_{\text{gluon}} \rangle / \langle n_{\text{quark}} \rangle = 1.06 \pm 0.05 \, .$$

6.7. Intermittency

The word 'intermittency' denotes local particle density fluctuations, as seen first in cosmic ray events, hadron-hadron collisions etc. [123, 124, and references therein]. The interest in studies of intermittency effects lies in the fact that Monte Carlo models can not describe most of these measurements.

It is therefore important to study intermittency also in e^+e^- events and to compare the results to the QCD models. This has been done for data taken at $\sqrt{s} \approx 30$ GeV with contradictory results: While the TASSO collaboration finds data and Monte Carlo predictions to be in disagreement [125], a recent CELLO study comes to the opposite conclusion [126]. Here the LEP results will be presented, which support the CELLO conclusions.

Intermittency is measured via factorial moments [127], which can be defined for one or more dimensions. Here the one-dimensional case is briefly described. To measure factorial moments one has to choose a phase space variable with a distribution which is approximately flat. Often one uses rapidity $y = -\frac{1}{2} \ln \frac{E - p_{\parallel}}{E + p_{\parallel}}$, which is calculated for each particle in an event. E and $p_{\parallel}$ denote the energy and the longitudinal momentum component with respect to the thrust axis. The rapidity interval Y which is considered in the analysis is then subdivided into M subintervals of size $\delta y = Y/M$. For each event one can count the number of particles n_m per bin and the total number of particles $N = \sum n_m$. The factorial moments of rank i are then defined as an average over many events in the following way:

$$F_i(\delta y) = \frac{M^{i-1}}{\langle N \rangle^i} \langle \sum_{m=1}^{M} n_m(n_m-1)\dots(n_m-i+1) \rangle$$

Note that only subintervals with at least i particles contribute to the factorial moments of rank i. The analysis must then be repeated for decreasing subinterval sizes δy (increasing resolution). The result may belong to one of the two classes [127]:

a) no correlation between particles: $F_i = \text{const}$

b) self similar cascades: $F_i \sim (\delta y)^{-f_i} \sim M^{f_i}$

Self similar cascades are indeed expected in $e^+e^- \to$ hadrons events, in which quark gluon cascades appear quite naturally. Of course this can be at most a qualitative picture. In addition, other effects like hard gluon radiation, fragmentation, Bose-Einstein correlations and particle decays (resonances, $\pi^0 \to e^+e^-\gamma$) can contribute to the rise of factorial moments with M.

ALEPH, DELPHI and OPAL have measured factorial moments for large data samples [128, 129, 130]. The ALEPH results for the factorial moments F_2–F_5 as function of the number of subdivisions of the rapidity interval are shown in figure 36 [128].

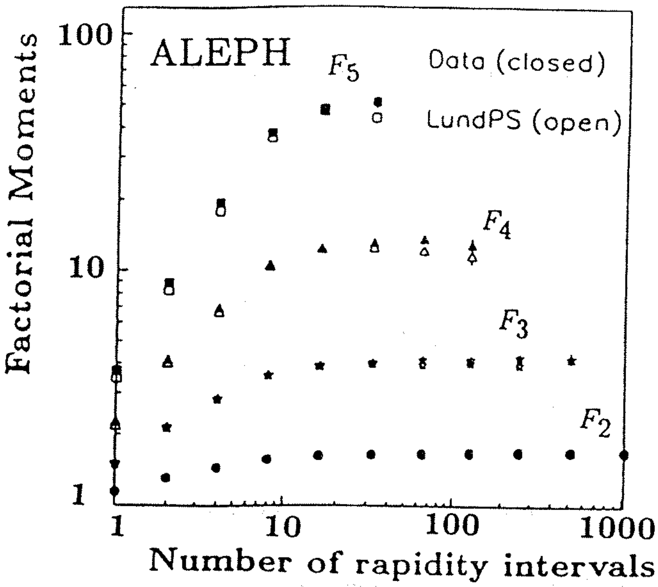

Figure 36: Factorial moments measured by ALEPH

At small M there is a rise with M, that implies the presence of local particle density fluctuations. The data can be reproduced by the JETSET parton shower Monte Carlo generator, therefore it can be explained by known physics. The main contribution to the rise of the moments in figure 36 stems from hard gluon emission.

Similar results have been obtained for different variables and also for analyses in more than one dimension.

The fact that for reactions other than e^+e^- the corresponding models do not reproduce the measurements [123] is probably due to the fact that those models are not yet as developed as the sophisticated generators used to simulate e^+e^- collisions.

6.8. Bose-Einstein correlations

Identical bosons obey Bose-Einstein statistics and prefer to occupy the same quantum state. This phenomenon has been studied at LEP for like sign charged pions by ALEPH [131], DELPHI [132] and OPAL [133]. Bose-Einstein correlations are described by a correlation function

$$C(p_1, p_2) = \frac{\rho(p_1, p_2)}{\rho(p_1) \cdot \rho(p_2)} .$$

Here $\rho(p_1, p_2)$ is the joined two-pion probability density and $\rho(p_i)$ denote the single pion probabilities. p_i are the particle four momenta. Assuming a pion source with a Gaussian shape in the rest frame of the pion pair, one obtains a correlation function of the form

$$C(Q) = 1 + \lambda \exp(-Q^2 \cdot r^2)$$

where $Q^2 = (p_1 - p_2)^2 = m^2(\pi\pi) - 4m_\pi^2$ and r is the source size. The parameter λ, which assumes values between 0 and 1, is a measure of the strength of the effect.

The principal experimental difficulty is the choice of a reference sample not affected by Bose-Einstein correlations in order to measure the product $\rho(p_1) \cdot \rho(p_2)$. One such reference sample consists of oppositely charged pions. A second method is based on event mixing. Finally Monte Carlo calculations not incorporating Bose-Einstein effects can be used.

Figure 37 shows the ratio of like sign and oppositely charged pions as a function of Q as measured by OPAL [133]. The data shown have been divided by the corresponding Monte Carlo correlation function (without Bose-Einstein effects) to correct for resonance decays. In addition a correction for final state Coulomb interactions has been applied.

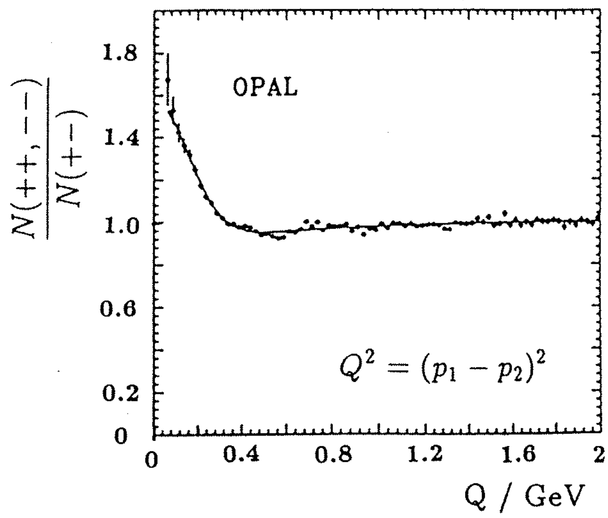

Figure 37: Bose-Einstein correlations measured by OPAL

The averaged results on correlation strength λ and source size r at LEP are shown in table 6 [134]. These values are *not* corrected for non pion contamination, which is estimated to be about 20%.

λ	0.5 ± 0.2
r/fm	0.8 ± 0.1

Table 6: Bose-Einstein correlation parameters

The parameters measured at LEP are not different from those measured in e^+e^- annihilation at lower center of mass energies. The same source size of about 1 fm describing the size of the hadronization region is also found for hadron-hadron and lepton-hadron collisions [134].

7. Future QCD studies at the Z^0

Future *experimental* progress will come mainly from an increase of statistics at the Z^0 resonance (a few million events) which will lead to the following improvements:

- The error in the ratio R_Z of the hadronic and leptonic Z^0 widths will be reduced, so that α_s can be determined with an uncertainty of about 5% from R_Z. This forecast assumes that each of the four experiments achieves systematic errors better than $\Delta R_Z/R_Z \approx 0.5\%$.
- Very important will be the study of multijet events using quark and flavor tagging, which works best for bottom events. However, since only a small fraction of all hadron events can be used, a large number of Z^0 events is needed. One can in particular repeat all matrix element tests as described in section 5 with identified (anti)quark and gluon jets.
- Interesting comparisons will become possible between the production of hard photons and gluons in hadronic events [135].
- More detailed studies of 'soft' phenomena will be performed, in particular of gluon coherence effects [87]. The study of particle yields including 'rare' hadrons and correlations will profit from a large increase in the event samples [136]. The search for 'anomalous' events, in particular those with exceptionally large factorial moments, will continue.

A further increase in the precision of α_s as determined from 3-jet like observables requires a major *theoretical* effort, namely QCD calculations of higher order corrections. For certain event shape variables (next to) leading logarithms have recently been calculated and resummed to all orders [137]. These corrections are due to soft and collinear gluons. However, a full third order matrix element calculation, which is needed for a precise prediction of hard gluon distributions, will not be accomplished very soon.

8. Summary and Conclusions

The experiments ALEPH, DELPHI, L3 and OPAL at LEP have performed a large number of measurements of the process $e^+e^- \rightarrow Z^0 \rightarrow$ hadrons with the following results:

- The strong coupling constant is found to be $\alpha_s = 0.120 \pm 0.007$ at the Z^0 mass. This number is an average of the values obtained from (i) the ratio of the hadronic and leptonic Z^0 widths and (ii) from analyzing the event topology. The strong coupling strength for bottom quarks is found to agree with that of the lighter quarks. The running of α_s, as predicted by QCD, is confirmed by the measured $\sqrt{s}$ dependence of the 3-jet fraction.
- Various distributions for 3-jet and 4-jet events have been measured precisely. They can be reproduced by QCD. Alternative models with scalar gluons or without gluon self interaction can be ruled out. The triple gluon coupling strength has been measured and is found to agree with QCD predictions.
- String and cluster fragmentation models describe hadronic events well. All distributions at the hadron level are reproduced by QCD Monte Carlo programs or analytical calculations. There is no evidence for any 'failure' of QCD in reproducing the LEP data.

The large number of studies of hadronic Z^0 decays at LEP have increased significantly our confidence in QCD as the theory of strong interactions.

9. Acknowledgements

I would like to thank my colleagues from the ALEPH, DELPHI and OPAL collaborations, in particular Siegfried Bethke, Wim de Boer, Jürgen Drees, Klaus Hamacher and Michael Schmelling, for helpful discussions, and for providing me with unpublished material. I am grateful to Albrecht Böhm, Martin Grünewald, Valery Khoze, Lalit Sehgal, Torbjörn Sjöstrand and Peter Zerwas for many clarifying comments.

10. References

[1] P. Roudeau, "Heavy Flavour Physics at LEP", this conference.

[2] G. Martinelli, "Status of QCD", this conference.

[3] ALEPH Collaboration, D. Decamp et al., *Nucl. Instrum. Methods* **A 294** (1990) 121.

[4] DELPHI Collaboration, P. Aarnio et al., *Nucl. Instrum. Methods* **A 303** (1991) 233.

[5] L3 Collaboration, B. Adeva et al., *Nucl. Instrum. Methods* **A 289** (1990) 35.

[6] OPAL Collaboration, K. Ahmet et al., *Nucl. Instrum. Methods* **A 305** (1991) 275.

[7] T. Sjöstrand in "Z Physics at LEP 1", CERN Report CERN-89-08, Vol.III., p. 143.

[8] T. Sjöstrand, *Comput. Phys. Commun.* **39** (1986) 347;
T. Sjöstrand and M. Bengtsson, *Comput. Phys. Commun.* **43** (1987) 367.

[9] R.K. Ellis, D.A. Ross and E.A. Terrano, *Nucl. Phys.* **B 178** (1981) 421.

[10] F. Gutbrod, G. Kramer, G. Schierholz, *Z. Phys.* **C 21** (1984) 235.

[11] G. Marchesini and B. Webber, *Nucl. Phys.* **B 310** (1988) 461;
I.G. Knowles, *Nucl. Phys.* **B 310** (1988) 571.

[12] U. Pettersson, "ARIADNE: A Monte Carlo for QCD Cascades in the Color Dipole Formulation", Lund Preprint LU TP 88-5;
L. Lönnblad, "ARIADNE 3: A Monte Carlo for QCD Cascades in the Color Dipole Formulation", Lund Preprint LU TP 89-10 (1988);
L. Lönnblad, "The Color Dipole Cascade Model and the Ariadne Program", Lund Preprint LU TP 91-11 (1991).

[13] K. Kato and T. Munehisa, "NLLjet: A Monte Carlo Code for e^+e^- QCD Jets including Next-to-Leading-Order Terms", CERN Preprint CERN-TH.5719/90.

[14] N. Magnussen, "Measurement of Jet Cross Sections in e^+e^- Annihilation at 44 GeV Center of Mass Energy", DESY Internal Report F22-89-01 (1989).

[15] Z. Kunszt and P. Nason in "Z Physics at LEP 1", CERN Report CERN-89-08, Vol.I., p. 373.

[16] ALEPH Collaboration, D. Decamp et al., *Phys. Lett.* **B 234** (1990) 209.
ALEPH Collaboration, D. Decamp et al., "Properties of Hadronic Z^0 Decays and Test of QCD Generators", ALEPH internal note, February 1991.

[17] DELPHI Collaboration, P. Aarnio et al., *Phys. Lett.* **B 240** (1990) 271;
DELPHI Collaboration, P. Abreu et al., "Comparison of Data with QCD Models", DELPHI note 91-74 PHYS 128, paper contributed to this conference.

[18] L3 Collaboration, B. Adeva et al., *Phys. Lett.* **B 257** (1991) 469.

[19] OPAL Collaboration, M.Z. Akrawy et al., *Z. Phys.* **C 47** (1990) 505.

[20] MARK II Collaboration, G.S. Abrams et al., *Phys. Rev. Lett.* **63** (1989) 1558;
MARK II Collaboration, G.S. Abrams et al., *Phys. Rev. Lett.* **64** (1990) 1334.

[21] G.G. Ross, "Beyond the Standard Model", this conference;
W. de Boer, "LEP data and Grand Unification", this conference.

[22] M. Aguilar-Benitez et al., *Phys. Lett.* **B 239** (1990) 1.

[23] L.R. Surguladze and M.A. Samuel, *Phys. Rev. Lett.* **66** (1991) 560;
S.G. Gorishny, A.L. Kataev and S.A. Larin, *Phys. Lett.* **B 259** (1991) 144.

[24] S. Barshay, P. Heiliger and L.M. Sehgal, *Z. Phys.* **C 49** (1991) 261.

[25] D. Bardin et al, program ZFITTER;
D. Bardin et al., *Nucl. Phys.* **B 351** (1991) 1;
D. Bardin et al., *Z. Phys.* **C 44** (1989) 493;
D. Bardin et al., *Phys. Lett.* **B 255** (1991) 290.

[26] T. Hebbeker, "QCD correction to Γ_{had}", Aachen Report PITHA 91/08 (revised version).

[27] B.A. Kniehl and J.H. Kühn, *Phys. Lett.* **B 224** (1989) 229;
B.A. Kniehl and J.H. Kühn, *Nucl. Phys.* **B 329** (1990) 547;
A. Djouadi, J.H. Kühn and P.M. Zerwas, *Z. Phys.* **C 46** (1990) 411;
K.G. Chetyrkin and J.H. Kühn, *Phys. Lett.* **B 248** (1990) 359.

[28] ALEPH Collaboration, D. Decamp et al., "Improved Measurement of Electroweak Parameters from Z Decays into Fermion Pairs", CERN Preprint CERN-PPE/91-105.

[29] DELPHI Collaboration, P. Abreu et al., "Determination of Z^0 Resonance Parameters and Couplings from its Hadronic and Leptonic Decays", CERN Preprint CERN-PPE/91-95, paper contributed to this conference.

[30] L3 Collaboration, B. Adeva et al., *Z. Phys.* **C 51** (1991) 179;
J. Alcaraz (L3 Collaboration), "Z Lineshape", this conference.

[31] OPAL Collaboration, G. Alexander et al., "Measurement of the Z^0 Line Shape Parameters and the Electroweak Coupling of Charged Leptons", CERN Preprint CERN-PPE/91-67, paper contributed to this conference.

[32] J. Carter, "Precision Tests of the Standard Model at LEP", this conference.

[33] L3 Collaboration, B. Adeva et al., *Phys. Lett.* **B 248** (1990) 464.

[34] JADE Collaboration, W. Bartel et al., *Z. Phys.* **C 33** (1986) 23;

JADE Collaboration, S. Bethke et al., *Phys. Lett.* **B 213** (1988) 235.

[35] OPAL Collaboration, M.Z. Akrawy et al., *Phys. Lett.* **B 235** (1990) 389;
OPAL Collaboration, M.Z. Akrawy et al., *Z. Phys.* **C 49** (1991) 375, paper contributed to this conference.

[36] G. Kramer, *Nucl. Phys.* **B 16** (Proc. Suppl.) (1990) 254.

[37] P.M. Stevenson, *Phys. Rev.* **D 23** (1981) 2916;
P.M. Stevenson, *Nucl. Phys.* **B 203** (1982) 472;
P.M. Stevenson, *Nucl. Phys.* **B 231** (1984) 65.

[38] G. Kramer and B. Lampe, *Fortschr. Phys.* **37** (1989) 161.

[39] G. Grunberg, *Phys. Lett.* **B 95** (1980) 70;
G. Grunberg, *Phys. Rev.* **D 28** (1983) 228.

[40] S.J. Brodsky, G.P. Lepage and P.B. Mackenzie, *Phys. Rev.* **D 28** (1983) 228.

[41] N. Brown and W.J. Stirling, *Phys. Lett.* **B 252** (1990) 657.

[42] ALEPH Collaboration, D. Decamp et al., *Phys. Lett.* **B 255** (1991) 623;
T. Lohse (ALEPH Collaboration), private communication.

[43] DELPHI Collaboration, P. Abreu et al., *Phys. Lett.* **B 247** (1990) 167, paper contributed to this conference;
K. Hamacher (DELPHI Collaboration), private communication.

[44] MARK II Collaboration, S. Komamiya et al., *Phys. Rev. Lett.* **64** (1990) 987.

[45] ALEPH Collaboration, D. Decamp et al., *Phys. Lett.* **B 257** (1991) 479.

[46] DELPHI Collaboration, P. Abreu et al., *Phys. Lett.* **B 252** (1990) 149;
K. Hamacher (DELPHI Collaboration), private communication.

[47] DELPHI Collaboration, P. Abreu et al., "Determination of α_s in Second Order QCD from Event Shapes Measured in Hadronic Z^0 Decays", DELPHI note 91-54 PHYS 109, paper contributed to this conference.

[48] OPAL Collaboration, M.Z. Akrawy et al., *Phys. Lett.* **B 252** (1990) 159, paper contributed to this conference.

[49] OPAL Collaboration, G. Azuelos, "Measurement of α_s from Planar Triple-Energy Correlations in Hadronic Decays of the Z^0", OPAL internal note PN032, March 1991.

[50] OPAL Collaboration, S. Sanghera, "A Measurement of $\alpha_s(M_Z)$ from C Planarity, Oblateness and Thrust at the Z^0 Peak", OPAL internal note PN033, April 1991.

[51] N. Magnoli, P. Nason and R. Rattazi, *Phys. Lett.* **B 252** (1990) 271.

[52] T. Hebbeker, "QCD at LEP/SLC", Aachen Report PITHA 91/11.

[53] S. Bethke, "Experimental Overview of Jet Physics and Tests of QCD", CERN Preprint CERN-PPE/91-36.

[54] J. Ellis, D.V. Nanopoulos and D.A. Ross, *Phys. Lett.* **B 267** (1991) 132.

[55] S. Bethke (OPAL Collaboration), private communication.

[56] L3 Collaboration, B. Adeva et al., *Phys. Lett.* **B 265** (1991) 451.

[57] G. Altarelli, *Annu. Rev. Nucl. Part. Sci.* **39** (1989) 357;
G. Altarelli, "QCD and Experiment", CERN Preprint CERN-TH 5760/90.

[58] A.D. Martin, R.G. Roberts and W.J. Stirling, *Phys. Rev.* **D 43** (1991) 3648;
A.D. Martin, R.G. Roberts and W.J. Stirling, *Phys. Lett.* **B 266** (1991) 173.

[59] A. Milsztajn, "α_s from Deep Inelastic Scattering", this conference.

[60] UA2 Collab., J. Alitti et al., *Phys. Lett.* **263** (1991) 563;
M. Lindgren et al., "A Measurement of the Strong Coupling Constant α_s in W Boson Production at the CERN Proton-Antiproton Collider", University of California Preprint UCR/UA1/91-01.

[61] G. d'Agostini, W. de Boer and G. Grindhammer, *Phys. Lett.* **B 229** (1989) 160;
R. Marshall, *Z. Phys.* **C 43** (1989) 595;
V. Branchina et al., *Phys. Rev. Lett.* **65** (1990) 3237.

[62] L3 Collaboration, B. Adeva et al., "Measurement of the Strong Coupling Constant α_s for Bottom Quarks at the Z^0 Resonance", L3 Preprint # 33 (1991).

[63] E. Gallo (L3 Collaboration), "Test of QCD Using 3-Jet Events and Measurement of $\alpha_s(b)$ with L3", this conference.

[64] TASSO Collaboration, W. Braunschweig et al., *Z. Phys.* **C 42** (1989) 17.

[65] N. Magnussen (JADE Collaboration), "Latest PETRA results on QCD", XX. Int. Symp. on Multiparticle Dynamics, Dortmund 1990; editors R. Baier and D. Wegener, World Scientific (1991) p. 273.

[66] TASSO Collaboration, W. Braunschweig et al., *Phys. Lett.* **B 214** (1988) 286;
MARK II Collaboration, S. Bethke et al., *Z. Phys.* **C 43** (1989) 325;
AMY Collaboration, I.H. Park et al., *Phys. Rev. Lett.* **62** (1989) 1713;
VENUS Collaboration, K. Abe et al., *Phys. Lett.* **B 240** (1990) 232.

[67] L3 Collaboration, B. Adeva et al., *Phys. Lett.* **263** (1991) 551.

[68] OPAL Collaboration, G. Alexander et al, "Measurement of Three-Jet Distributions Sensitive to the Gluon Spin in e^+e^- Annihilations at $\sqrt{s}$ = 91 GeV", CERN Preprint CERN-PPE/91-97, paper contributed to this conference.

[69] DELPHI Collaboration, P. Abreu et al., "Study of Orientation of 3-jet Events in Z^0 Hadronic Decays", CERN Preprint CERN-PPE/91-79.

[70] E. Laermann, K.H. Streng and P.M. Zerwas, *Z. Phys.* **C 3** (1980) 289,
E. Laermann, K.H. Streng and P.M. Zerwas, to be publ. in *Z. Phys.* C (Erratum);
K. Koller et al., *Z. Phys.* **C 6** (1980) 131.

[71] J.G. Körner, G.A. Schuler and F. Barreiro, *Phys. Lett.* **B 188** (1987) 272;
G.A. Schuler and J.G. Körner, *Nucl. Phys.* **B 325** (1989) 557.

[72] K. Koller and H. Krasemann, *Phys. Lett.* **B 88** (1979) 119;
UA1 Collaboration, G. Arnison et al., *Phys. Lett.* **B 136** (1984) 294;
UA2 Collaboration, P. Bagnaia et al., *Phys. Lett.* **B 144** (1984) 283;
N. Artega-Romero, A. Nicolaidis and J. Silva, *Phys. Rev. Lett.* **52** (1984) 172.

[73] TASSO Collaboration, R. Brandelik et al., *Phys. Lett.* **B 97** (1980) 453;
D. Lüke (TASSO Collaboration), "Recent Results from TASSO", Proceedings of the 21st International Conference on High Energy Physics, Paris (1982);
PLUTO Collaboration, C. Berger et al., *Phys. Lett.* **B 97** (1980) 459;
CELLO Collaboration, H.-J. Behrend et al., *Phys. Lett.* **B 110** (1982) 329;
R. Clare (MARK J Collaboration), "QCD Properties of Jets", MIT Ph.D. Thesis (1982), unpublished.

[74] K.J.F. Gaemers and J.A.M. Vermaseren, *Z. Phys.* **C 7** (1980) 81.

[75] J.G. Körner, G. Schierholz and J. Willrodt, *Nucl. Phys.* **B 185** (1981) 365.

[76] O. Nachtmann and A. Reiter, *Z. Phys.* **C 16** (1982) 45;
G. Rudolph in "Physics at LEP", CERN Report CERN-86-02, Vol.II., p. 150.

[77] M. Bengtsson and P.M. Zerwas, *Phys. Lett.* **B 208** (1988) 306.

[78] S. Bethke, A. Ricker and P.M. Zerwas, *Z. Phys.* **C 49** (1991) 59.

[79] L3 Collaboration, B. Adeva et al., *Phys. Lett.* **B 248** (1990) 227.

[80] OPAL Collaboration, M.Z. Akrawy et al., *Z. Phys.* **C 49** (1991) 49.

[81] R. Itoh, "Recent Results from TRISTAN", this conference.

[82] L. DiLella, *Annu. Rev. Nucl. Part. Sci.* **35** (1985) 107.

[83] ALEPH Collaboration, D. Decamp et al., "Testing the Non-Abelian Structure of QCD Based on Four-Jet Events - Evidence for the Triple Gluon Vertex", ALEPH internal note 91-84, June 1991.

[84] DELPHI Collaboration, P. Abreu et al., *Phys. Lett.* **B 255** (1991) 466;
DELPHI Collaboration, P. Abreu et al., "Evidence for the Triple-Gluon Vertex by Measuring the Color-Factor", DELPHI note 91-52 PHYS 107, paper contributed to this conference.

[85] D. Salmon (ALEPH Collaboration), "Studies of the Triple Gluon Vertex with ALEPH", this conference.

[86] A.H. Mueller, *Phys. Lett.* **B 104** (1981) 161;
A. Bassetto et al., *Nucl. Phys.* **B 207** (1982) 189;
B.I. Ermolaev and V.S. Fadin, *JETP Lett.* **33** (1981) 285;
Y.L. Dokshitzer, V.S. Fadin and V.A. Khoze, *Phys. Lett.* **B 115** (1982) 242.

[87] V.A. Khoze, "Color Coherence Physics at the Z^0", CERN Preprint CERN-TH 5849-90;
V.A. Khoze, Y.L. Dokshitzer and S.I. Troyan, "Color Coherence in QCD Jets", Lund Preprint LU TP 90-12.

[88] V. Khoze and L. Lõnnblad, *Phys. Lett.* **B 241** (1990) 123.

[89] D. Amati and G. Veneziano, *Phys. Lett.* **B 83** (1979) 87.

[90] Y.L. Dokshitzer and S.I. Troyan, "Non-leading Perturbative Corrections to the Dynamics of Quark-Gluon Cascades and Soft Hadron Spectra in e^+e^- Annihilation", Leningrad Preprint LNPI-922 (1984);
Y.I. Azimov et al., *Z. Phys.* **C 27** (1985) 65;
Y.I. Azimov et al., *Z. Phys.* **C 31** (1986) 213.

[91] ALEPH Collaboration, D. Decamp et al., "Measurement of the Charged Particle Multiplicity Distribution in Hadronic Z Decay", CERN Preprint CERN-PPE/91-159.

[92] DELPHI Collaboration, P. Aarnio et al., "Charged Multiplicity and Rapidity Distributions in Z^0 Hadronic Decays", CERN Preprint CERN-PPE/90-117, paper contributed to this conference;
DELPHI Collaboration, P. Abreu et al., *Z. Phys.* C 50 (1991) 185;
DELPHI Collaboration, P. Abreu et al., " Charged Particle Multiplicity Distributions in Restricted Rapidity Intervals in Z^0 Hadronic Decays" CERN Preprint CERN-PPE/91-78, paper contributed to this conference;
DELPHI Collaboration, P. Abreu et al., "Multiplicity Dependence of Mean Transverse Momentum in e^+e^- Annihilations at LEP Energies", DELPHI note 91-59 PHYS 114, paper contributed to this conference.

[93] L3 Collaboration, B. Adeva et al., *Phys. Lett.* **B 259** (1991) 199.

[94] S. Carius and G. Ingelman, *Phys. Lett.* **B 252** (1990) 647;
R. Szwed, G. Wrochna and A.K. Wróblewski, *Mod. Phys. Lett.* **A 5** (1990) 1851.

[95] E.D. Malaza and B.R. Webber, *Phys. Lett.* **B 149** (1984) 501;
E.D. Malaza and B.R. Webber, *Nucl. Phys.* **B 267** (1986) 702.

[96] K.Tesima, *Phys. Lett.* **B 221** (1989) 91;
F. Cuypers and K. Tesima, *Z. Phys.* **C 52** (1991) 69.

[97] Z. Koba, H.B. Nielsen and P. Olesen, *Nucl. Phys.* **B 40** (1972) 317.

[98] B. Loerstad (DELPHI Collaboration), "Charged Multiplicities and their Dependences Measured by DELPHI", this conference.

[99] DELPHI Collaboration, P. Abreu et al., "Charged Particle Multiplicity of Quarks and Gluon Jets in Z^0 Hadronic Decays", DELPHI note 91-58 PHYS 113, paper contributed to this conference.

[100] B.R. Webber, *Phys. Lett.* **B 143** (1984) 501.

[101] OPAL Collaboration, G. Alexander et al., *Phys. Lett.* **B 264** (1991) 467.

[102] DELPHI Collaboration, P. Abreu et al., "Production of K^0 and $K^{*\pm}$ in the Hadronic Decays of the Z^0", DELPHI note 91-56 PHYS 111, paper contributed to this conference.

[103] DELPHI Collaboration, P. Abreu et al., "Preliminary Results for Inclusive Λ Production in the Hadronic Decays of the Z^0", DELPHI note 91-64 PHYS 118, paper contributed to this conference.

[104] D.H. Saxon in "High Energy Electron Positron Physics" editors A. Ali and P. Söding, World Scientific (1988) p. 540.

[105] A.H. Mueller, *Nucl. Phys.* **B 213** (1983) 85,
A.H. Mueller, *Nucl. Phys.* **B 241** (1984) 141 (Erratum).

[106] C.P. Fong and B.R. Webber, *Phys. Lett.* **B 229** (1989) 289.

[107] V.A. Khoze, "Particle Distributions in Jets", this conference.

[108] D. Boutigny (L3 Collaboration), "Soft Gluon Coherence Effect in Inclusive Particle Spectra", this conference.

[109] ALEPH Collaboration, D. Decamp et al., "Measurement of Charged Particle Distributions Sensitive to QCD Coherence in Hadronic Z Decays", ALEPH internal note 91-103, July 1991.

[110] OPAL Collaboration, M.Z. Akrawy et al., *Phys. Lett.* **B 247** (1990) 617.

[111] V.A. Khoze and Y.L. Dokshitzer, private communication.

[112] P. Mazzanti and R. Odorico, "On a Recent OPAL Study of QCD Coherence Effects in Particle Momentum Spectra", Bologna Preprint DFUB 91/4.

[113] JADE Collaboration, W. Bartel et al., *Phys. Lett.* **B 101** (1981) 129;
JADE Collaboration, W. Bartel et al., *Z. Phys.* **C 21** (1983) 37.

[114] B. Andersson and G. Gustafson, *Phys. Lett.* **B 94** (1980) 211.

[115] P.M. Zerwas, "QCD, $\gamma\gamma$ and Heavy Quarks in e^+e^- Collisions", Aachen Report PITHA 89/23.

[116] T. Sjöstrand, "QCD and Jets at LEP", CERN Preprint CERN-TH/90-5902.

[117] OPAL Collaboration, M.Z. Akrawy et al., *Phys. Lett.* **B 261** (1991) 334, paper contributed to this conference.

[118] OPAL Collaboration, G. Alexander et al., *Phys. Lett.* **B 265** (1991) 462, paper contributed to this conference.

[119] M. Turner (OPAL Collaboration), "Observation of the String Effect and of Quark/Gluon-Jet Differences Using Quark Tagging at OPAL", this conference.

[120] Y.L. Dokshitzer at al., *Phys. Lett.* **B 245** (1990) 243.

[121] DELPHI Collaboration, P. Abreu et al., "Interjet Correlations in Hadronic Jets from Z^0 Decays", DELPHI note 91-53 PHYS 108, paper contributed to this conference.

[122] R. Odorico, *Comput. Phys. Commun.* **32** (1984) 139;
R. Odorico, *Comput. Phys. Commun.* **59** (1990) 527.

[123] W. Kittel, "Experimental Results on Intermittency", XX. Int. Symp. on Multiparticle Dynamics, Dortmund 1990; editors R. Baier and D. Wegener, World Scientific (1991) p. 401.

[124] A. Białas, "Theory of Intermittency", XX. Int. Symp. on Multiparticle Dynamics, Dortmund 1990; editors R. Baier and D. Wegener, World Scientific (1991) p. 669.

[125] TASSO Collaboration, W. Braunschweig et al., *Phys. Lett.* **B 231** (1989) 548.

[126] CELLO Collaboration, H.J. Behrend et al., *Phys. Lett.* **B 256** (1991) 97.

[127] A. Białas and R. Peschanski, *Nucl. Phys.* **B 273** (1986) 703;
A. Białas and R. Peschanski, *Nucl. Phys.* **B 308** (1988) 857.

[128] ALEPH Collaboration, D. Decamp et al., "An Investigation into Intermittency", CERN Preprint CERN-PPE/91-121.

[129] DELPHI Collaboration, P. Aarnio et al., *Phys. Lett.* **B 247** (1990) 137.

[130] OPAL Collab., M.Z. Akrawy et al., *Phys. Lett.* **262** (1991) 351, paper contributed to this conference.

[131] ALEPH Collaboration, D. Decamp et al., "A Study of Bose-Einstein Correlations in e^+e^- Annihilation at 91 GeV", ALEPH internal note, June 1991.

[132] DELPHI Collaboration, P. Abreu et al., "Bose-Einstein Correlations at LEP", DELPHI note 91-57 PHYS 112, paper contributed to this conference.

[133] OPAL Collaboration, P.D. Acton et al., *Phys. Lett.* **B 267** (1991) 143.

[134] S. Marcellini (OPAL Collaboration), "Bose-Einstein Correlations in High Energy Collisions", this conference.

[135] ALEPH Collaboration, D. Decamp et al., *Phys. Lett.* **B 264** (1991) 476;
DELPHI Collaboration, P. Abreu et al., "Study of Final State Photons in Hadronic Z^0 Decay and Limits on New Phenomena", DELPHI note 91-46 PHYS 101, paper contributed to this conference;
L3 Collaboration, B. Adeva et al., "Measurement of Final State Photon Radiation in Hadronic Z^0 Decays", L3 internal note 971, July 1991;
OPAL Collaboration, M.Z. Akrawy et al., *Phys. Lett.* **B 246** (1990) 285, paper contributed to this conference.

[136] I. Bergström et al., "Report of the Working Group on High Luminosity at LEP", CERN Report CERN-91-02, p. 182.

[137] S. Catani et al., *Phys. Lett.* **B 263** (1991) 491;
S. Catani, G. Turnock and B.R. Webber, "Heavy Jet Mass Distribution in e^+e^- Annihilation", CERN Preprint CERN TH.6231/91.